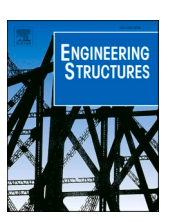
ELSEVIER

Contents lists available at ScienceDirect

# **Engineering Structures**

journal homepage: www.elsevier.com/locate/engstruct





# A consistent safety format and design approach for brittle systems and application to textile reinforced concrete structures

Qianhui Yu<sup>a,\*</sup>, Patrick Valeri<sup>a,b</sup>, Miguel Fernández Ruiz<sup>a,c</sup>, Aurelio Muttoni<sup>a</sup>

- <sup>a</sup> Ecole Polytechnique Fédérale de Lausanne, Switzerland
- <sup>b</sup> Dr. Lüchinger+Meyer Bauingenieure AG, Switzerland
- <sup>c</sup> Universidad Politécnica de Madrid, Spain

# ARTICLE INFO

Keyword:
Safety format
Brittle response
Statically indeterminate system
Action effect model uncertainty
Textile Reinforced Concrete
Tests

# ABSTRACT

Design and verification of structures in modern codes of practice account for a safety format, ensuring that the probability of failure does not exceed a given threshold. Although specific safety formats are proposed in some cases for special types of structures or analyses, most designs and verifications are currently performed on the basis of the Partial Safety Factor Format (PSFF). This format is applied to cover different materials and structural responses, allowing for a uniform methodology to account for reliability. Such consideration greatly simplifies the design process, but raises concerns on its consistency when different structural responses are observed. In the PSFF as considered in *fib* Model Code and Eurocodes, no explicit distinction is made on the value of the partial safety factors (for actions or materials) depending on whether a structural system has a brittle or a ductile response. This can be potentially inconsistent, as brittle systems have limited or no redistribution capacity of internal forces (which can give rise to premature failures if action effects are poorly estimated), while ductile systems have large potentials to redistribute internal forces and are thus little sensitive to this issue.

In this paper, to investigate on the suitability of PSFF for brittle structures, the most suitable manner to determine internal forces for brittle elements failing in bending and the corresponding model uncertainties of action effects are investigated in detail. The concepts are derived from a theoretical perspective and applied to the case of Textile Reinforced Concrete (TRC). This material is a promising development to reduce the footprint of concrete construction and to build lightweight structures, but exhibits a very brittle response in bending (contrary to ordinary reinforced concrete with usual reinforcement ratios). In this paper, by means of an experimental and theoretical investigation, it is shown that following a suitable approach to estimate internal forces for brittle systems as TRC leads to a low level of model uncertainty of action effects. This leads to the conclusion that, compared to standard design of ductile systems, no additional correction is required for safety issues. Following this outcome, the partial factors for TRC structures are calibrated. In addition, due to the significance of geometrical uncertainties, a method for designing TRC on the basis of a design value of the effective depth (a reduced value accounting for construction tolerances instead of its nominal dimension) is eventually discussed, showing that it allows for a more uniform level of safety.

### 1. Introduction

In the last decades, Textile Reinforced Concrete (TRC) has emerged as an interesting alternative to reinforced concrete, allowing to reduce material consumption and the carbon footprint of cementitious-based materials [1–3]. This new paradigm relies on the use of a non-metallic fabric as reinforcement (typically made of carbon or glass), which is insensitive to corrosion. As a consequence, cover requirements of the reinforcement can be reduced to minimum static values, allowing to

decrease the overall thickness of TRC elements to 10–30 mm. In addition, since no passivation of the reinforcement is required, a low-clinker content cement can also be used allowing to reduce the environmental footprint of the material related to its  ${\rm CO_2}$  emissions.

Despite the potential of TRC, its practical use remains still limited. This is to a large extent explained by the lack of a consistent design framework. Conventional methods widely accepted for reinforced concrete are potentially not directly applicable to TRC due to its brittle nature. This issue is particularly instrumental in the case of statically indeterminate structures, where redistributions of internal forces are

E-mail address: qianhui.yu@epfl.ch (Q. Yu).

<sup>\*</sup> Corresponding author.

Nomen	clature	$d_{max}$	maximum value of the flexural depth of all the rovings in a cross section
Latin up	per case letters	$d_{min}$	minimum value of the flexural depth of all the rovings in a
$A_{tex}$	total area of textile reinforcement in a beam cross section	··nut	cross section
$A_R$	coefficient in the multiplicative form approximation of the	$d_{design}$	design value for the flexural depth
K	resistance function	$d_{nom}$	nominal value for the flexural depth
$E_{calc}$	calculated action effect at a given cross section of a	$e_{tex}$	grid spacing of the textile reinforcement
cuic	structure	$f_c$	the compressive strength of concrete (motar)
$E_{cm}$	mean value of the elastic modulus of concrete (motar)	$f_{c,ck}$	characteristic value for concrete (motar) compressive
$E_{exp}$	experimental action effect at a given cross section of a	JUJUK	strength
ωр	structure	$f_{cm}$	mean value of the compressive strength of concrete
$E_d$	design value of action effect	Juni	(motar)
$E_{tex,m}$	mean value of the elastic modulus of textile reinforcement	$f_{ctm}$	mean value of the tensile strength of the concrete (motar)
	$EI_{UC}$ fully cracked and uncracked flexural rigidity of a cross	$f_{tex}$	the textile reinforcement tensile strength
10	section	$f_{tex,ck}$	characteristic value of the textile reinforcement tensile
F	load applied to a tested beam	•,	strength
$F_{rep}$	representative value of action variables	$f_{tex,d}$	design value of the textile reinforcement tensile strength
L	span of a beam	$f_{tex,m}$	mean value of the textile reinforcement tensile strength
$L_{01}$ and	$L_{o2}$ overhang of a beam in three point bending test	g()	performance function
M	bending moment of a cross section	h	height of a beam cross section
$M_I$	bending moment of a cross section of beam BI	$n_r$	number of textile rovings in a cross section
$M_{II}$	bending moment of a cross section of beam BII	$q_{calc}$	the calculated global resistance of a statically
$M_{cr}$	cracking moment of a cross section	Teute	indeterminate structure in terms of load factor
$M_{exp}$	ultimate bending resistance of a tested beam	$q_{cr,hog}$	external load level when the hogging region of a beam
$M_{hogging}$	maximum hogging moment of a beam according to a linear	Termog	cracks
nogguig	response	$q_{cr,sag}$	external load level when the sagging region of a beam
$M_{sagging}$	maximum sagging moment of a beam according to a linear	Terrsug	cracks
sugging	response	$q_E$	external action
$M_{R,hog}$	resistance of a beam cross section to the hogging moment	$q_{exp}$	experimental global resistance of a statically indeterminate
$M_{R,sag}$	resistance of a beam cross section to the sagging moment	техр	structure in terms of load factor
Prob ()	probability function	$q_{R,hog}$	external load level when the hogging region of a beam
Q	load applied to an assembled cross-beam system	1191108	reaches the ultimate resistance
	$Q_B$ load transferred to a component beam of an assembled	$q_{R,sag}$	external load level when the sagging region of a beam
Ci · ·	cross-beam system	Trysug	reaches the ultimate resistance
$Q_{exp}$	experimental resistance of an assembled cross-beam	$q_{R,I}$	external load level when beam BI reaches its load carrying
cusp	system	1.9.	capacity
$Q_{LAFC}$	resistance calculated with Linear Analysis assuming Fully-	$q_{R,II}$	external load level when beam BII reaches its load carrying
	Cracked stiffness (LAFC)	2-9	capacity
$Q_{LAUC}$	resistance calculated with Linear Analysis assuming	$x_N$	position of the neutral axis of a cross section
	UnCracked stiffness (LAUC)		
$Q_{NLA}$	resistance calculated with NonLinear Analysis (NLA)	Greek upp	per case letters
$R_{calc}$	calculated local resistance of a structure	$\Delta_d$	reduction factor for the flexural depth
$R_{exp}$	experimental local resistance of a structure	$\phi O$	cumulative distribution function of standardized Normal
$R_d$	design value of resistance		distribution
$U_{tex}$	nominal perimeter of the roving of textile reinforcement	Crook low	ver case letters
$V_d$	Coefficient of Variant (CoV) of the flexural depth random		FORM sensitivity factor of the flexural depth random
	variable	$\alpha_d$	variable
$V_{ftex}$	CoV of the textile reinforcement tensile strength random	α-	FORM sensitivity factor for action effects
<b>3</b>	variable	$\alpha_E$	FORM sensitivity factor of the textile reinforcement
$V_R$	CoV of the resistance random variable	$\alpha_{ftex}$	
$V_{Sd}$	CoV of the action effect model uncertainty	O4	strength random variable
$V_{ heta R}$	CoV of the model uncertainty of local resistance	$lpha_{ heta}$	FORM sensitivity factor of the model uncertainty of local
$X_k$	the characteristic value for a material strength variable	Ø-	resistance random variable FORM sensitivity factor for the resistance
$X_{num}$	the design vector for a component beam in the numerical	$\alpha_R$	· · · · · · · · · · · · · · · · · · ·
	cross-beam system study	$\beta_{achieved}$	achieved reliability index
			achieved reliability index for safety format proposal I
Latin lov	ver case letters	$\beta_{achieved}, II$	
$a_{nom}$	nominal value of geometrical variables	$\beta_{tgt}$	the target reliability index
$a_{tex}$	net cross section of the roving of textile reinforcement	$\beta_{tgt,50}$	the target reliability index for a reference period of 50
b	width of a beam cross section		years
d	flexural depth of a roving in a cross section	$\gamma_C$	partial factor for concrete compressive strength
$d_{ave}$	average flexural depth of all the rovings in a cross section	$\gamma_F$	partial factors applied to action variables

γ <sub>M</sub>	partial factors applied to material strength variables	$\theta_E$	random variable for action effect model uncertainty
γ <sub>Sd</sub>	partial factors for action effect model uncertainty	$\theta_{E,LAFC}$	action effect model uncertainty variable for LAFC
$\gamma_{tex,I}$	partial factor for textile reinforcement strength in safety	$\theta_{E,LAFC,num}$	action effect model uncertainty variable for LAFC
· ·	format Proposal I		evaluated with numerical method
$\gamma_{tex.II}$	partial factor for textile reinforcement strength in safety	$\theta_{E,LAUC}$	action effect model uncertainty variable for LAUC
,	format Proposal II	$\theta_{E,LAUC,num}$	action effect model uncertainty variable for LAUC
δ	mid-span deflection of a structure		evaluated with numerical method
$\delta_{cal}$	calculated mid-span deflection of a structure	$\theta_{E,NLA}$	action effect model uncertainty variable for NLA
$\delta_{exp}$	experimental mid-span deflection of a structure	$ heta_{global}$	random variable for the global resistance model
$\epsilon_c$	strain of concrete		uncertainty
$\varepsilon_i$	strain of a single textile reinforcement roving	$\theta_{R,local}$	random variable for the local resistance model uncertainty
η	mean value of the conversion factors for material strength	$\rho$	flexural reinforcement ratio of a cross section
	variables	$\rho_{ave}$	average flexural reinforcement ratio of a cross section
$\eta_E$	efficiency factor for the textile modulus of elasticity	$\sigma_c$	stress of concrete
$\eta_f$	efficiency factor for the textile tensile strength	$\sigma_i$	stress of a single textile reinforcement roving
$\eta_{is}$	the in-situ strength efficient factor of concrete	χ	curvature of a cross section

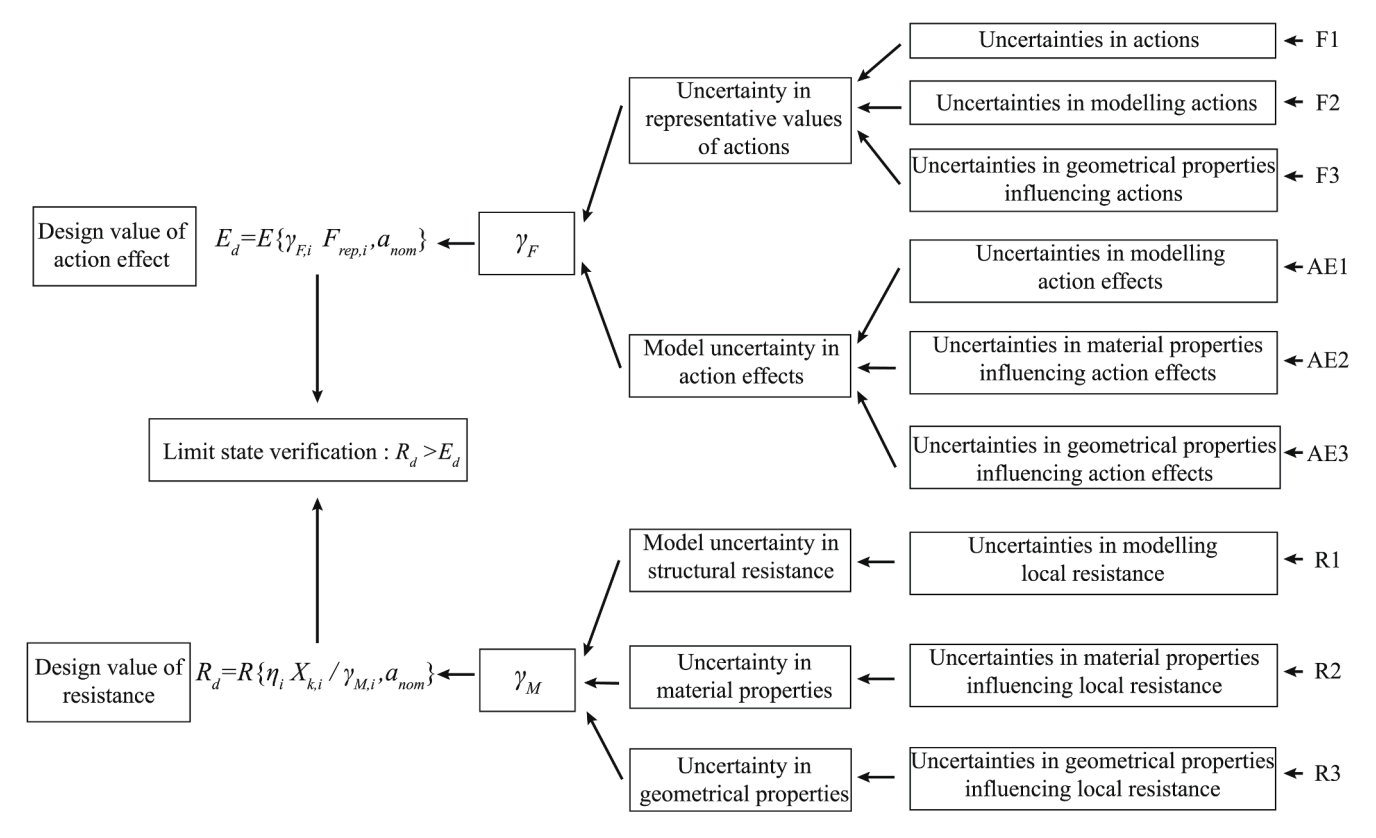


Fig. 1. Relation between individual partial factors (adapted from EN1990:2002 [9], refer to Nomenclature section for details).

usually required to develop the full structural strength of the system. Other aspects that are critical for the application of TRC in practice are the potential sensitivity of thin elements to construction tolerances and its reduced resistance in case of fire [4–6].

Currently, several analytical and numerical models are available to describe the response of TRC members with respect to its sectional behaviour. An extensive review of the state-of-the-art can be consulted elsewhere (see for instance [7,8]). These approaches refer normally to mean material properties and allow determining the average resistance of TRC structural elements (or with a bias factor which should be close to 1.0). However, their application in practice requires accounting for the inevitable uncertainties inherent to structural design. As a consequence, a suitable safety format needs to be implemented, ensuring that the probability of failure does not exceed an acceptable threshold. In the

case of the resistance formulae, such format shall account for the variability of the material properties as well as uncertainties related to the calculation model and to construction tolerances.

For the reliability verification of structures, the so-called Partial Safety Factor Format (PSFF) is adopted in many design codes (Eurocodes [9,10] and fib Model Code [11] for example). In the PSFF, design values of the basic variables are defined through partial safety factors and limit state verifications are made with the design values of basic variables [9]. Partial factors for different materials and actions need to be calibrated so that the reliability levels for representative structures in design are as close as possible to the target reliability level. With respect to the adoption of a suitable safety format for TRC design, several efforts have been performed in the past [12–17] to address the principles of structural reliability and design procedures.

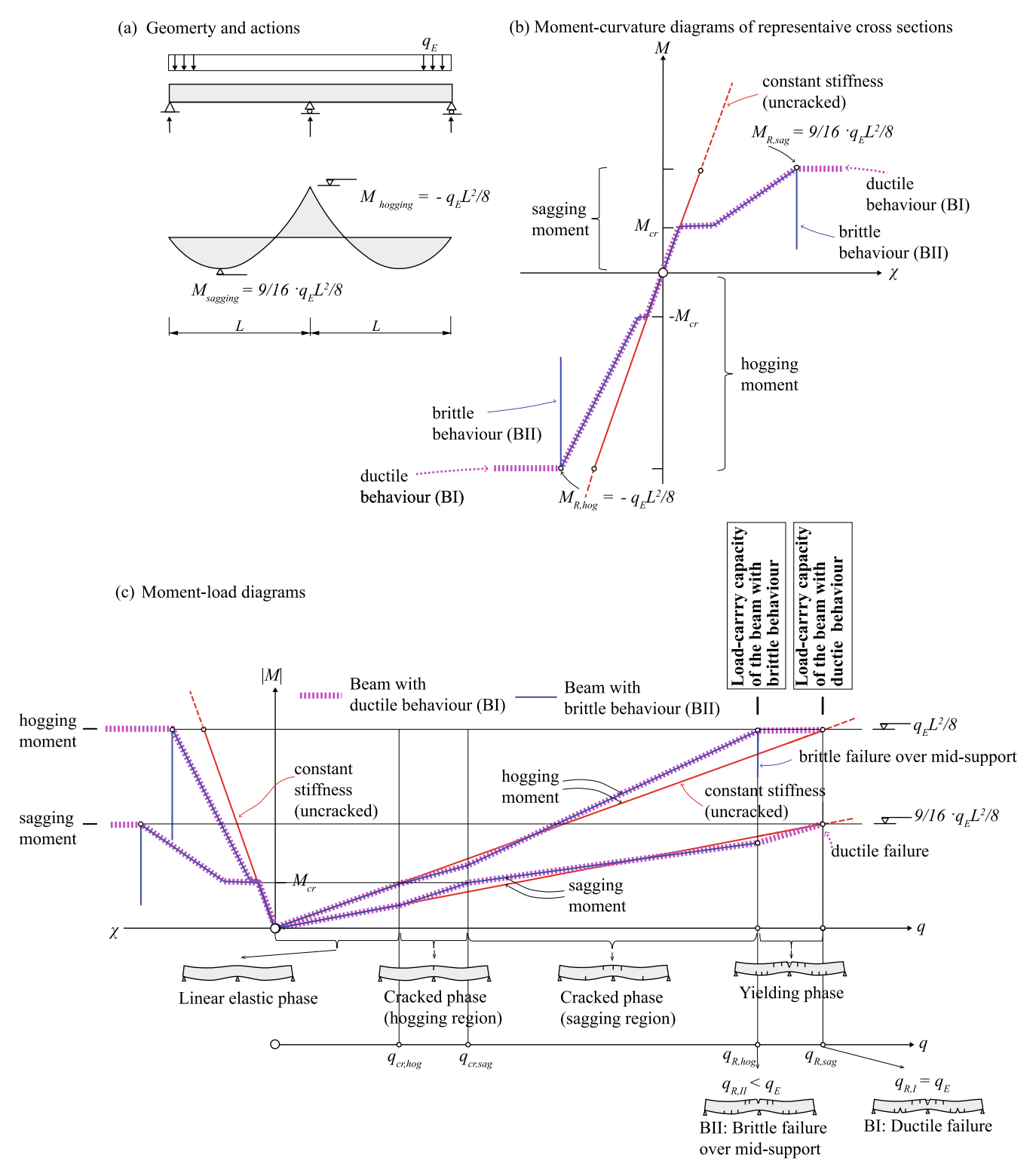


**Fig. 2.** Analysis of a statically indeterminate reinforced concrete structure designed according to the internal forces calculated assuming linear uncracked behaviour: (a) geometry and actions; (b) moment – curvature diagrams; and (c) moment – load diagrams.

The relationship between individual partial factors in PSFF of Eurocodes is shown in Fig. 1 (adapted from Figure C3 in EN1990:2002 [9] accounting for the new definitions in the draft of the second generation of prEN1990:2020 [18]). It should be noted that in addition to the basic uncertainties listed in Fig. 1, the partial safety factors should also account for approximations and uncertainties in the safety format calibration. Also, it has to be noted that this figure describes the classical

verification method for structures, where the analysis (calculation of internal forces) is conducted separately from the calculation of the associated resistances. Within this frame, the verification is conducted at a given cross section by comparison of sectional internal forces and related resistances. Such procedure will be referred in the following as a local verification. As an alternative, the distribution of internal forces can be calculated considering the response and strength of the materials

(following a nonlinear analysis). This allows to determine directly the load-carrying capacity of the system and will be referred to in the following as a global verification method. In this case, the quantification of the model uncertainties [19] can be quite different and other safety formats [9,11] can be more appropriate.

In Eurocodes [9], the partial factors of actions  $\gamma_F$  and the partial factors of material strength variables  $\gamma_M$  are typically calibrated separately by using constant standardised First Order Reliability Method (FORM) sensitivity factors [9,20,21]. Taking advantage of this frame, in order to define a safety format for TRC structures, only the partial factors related to the resistance (materials) need to be recalibrated, while the partial factors for action variables from Eurocodes [9] can theoretically be maintained.

It is interesting to note in Fig. 1 that the model uncertainty of action effects is accounted for in the partial factor for action variables,  $\gamma_F$ . Such assumption, provided that a constant value of  $\gamma_F$  is adopted, ignores differences related to material response (brittle/ductile response) and analysis method (linear-elastic response/consideration of redistributions). This simplification can lead to unsatisfactory levels of reliability for statically indeterminate brittle structures (as those built with TRC).

In this paper, the action effect model uncertainty of TRC structures will be investigated on the basis of a statistical evaluation of the results of an experimental programme designed for this purpose. This investigation will focus not only on statically determinate elements, but also on the response of statically indeterminate structures failing in a brittle manner. The safety format and partial factor related to the resistance ( $\gamma_M$ ) for TRC structures will then be calibrated based on a proper probabilistic modelling of the basic variables. A suitable model to account for action effects on TRC structures and the corresponding model uncertainty will be presented. On its basis, tailored values of the partial safety factors for TRC will be derived as well as a suitable design approach for calculation of internal forces.

# 2. Action effect model uncertainty in statically indeterminate structures

In this section, the different influences of brittle and ductile responses on statically indeterminate structures are examined with respect to their mechanical consequences and the associated reliability considerations.

# 2.1. Influence of sectional behaviour on the structural response

To illustrate the different model uncertainty of action effects of structures with different sectional response (brittle/ductile), the load-bearing behaviour of statically indeterminate structures with different materials is first investigated. As a representative example, two beams with identical geometry and loading conditions (see Fig. 2a) but whose material response is different are examined:

- Beam BI refers to the classical response of concrete reinforced with ordinary steel rebars. Its moment-curvature diagram can be approximated by a quadrilinear law showing a plastic plateau with large deformation capacity related to extensive yielding of the longitudinal reinforcement and significant ultimate strain of the reinforcement steel (see Fig. 2b). This response can be considered as ductile and thus insensitive to imposed deformations (allowing to calculate the structural capacity according to limit analysis [22]).
- Beam BII refers to a structure reinforced with a brittle reinforcement, as for TRC, whose failure occurs prior to any plastic plateau or to an over-reinforced structure with conventional steel reinforcement where the compression zone crushes before the reinforcement yields.
   The capacity to redistribute internal forces is limited to the change of stiffness related to the cracked response and the structure can

potentially be sensitive to imposed deformations (limit analysis not applicable to calculate its structural capacity).

In a classical design of a reinforced concrete structure, the internal forces are calculated assuming linear uncracked behaviour (not considering cracking nor yielding). This allows neglecting the influence of the reinforcement on the stiffness, so that no iteration is required in designing a new structure. In this case, the sections of the beam described above would be designed so to resist for the external action  $(q_E)$  both the maximum sagging moment according to a linear response  $(M_{R,sag} = 9/16 \cdot q_E L^2/8)$  and the maximum hogging moment  $(M_{R,hog} = -1)$  $q_E L^2/8$ ), requiring thus different amount of reinforcement at these sections, see Fig. 2b. In reality, when the load is applied, different phases of response can be observed as shown in Fig. 2c for the two characteristic sections (hogging and sagging region). Before cracking occurs, the distribution of bending moments follows that of the elastic uncracked behaviour, with proportional increments to the load at both control sections (maximum sagging moment equal to  $9/16 \cdot qL^2/8$  and a maximum hogging moment equal to  $-qL^2/8$ ). Cracking occurs first in the hogging region ( $q_{cr,hog}$  in Fig. 2c), leading to a local loss of stiffness. As a consequence, bending moments increase more than proportionally in the sagging region and less than proportionally in the hogging region.

For a higher level of load, cracking at the sagging region also occurs  $(q_{cr,sag})$  and the internal forces redistribute thereafter according to the relative stiffness of the hogging and sagging regions. Since the reinforcement in the hogging region is higher due to the design procedure (Fig. 2b), its stiffness is also higher and moments increase more than proportionally in the hogging region (Fig. 2c). Depending on the strength, the hogging or sagging region can first attain their strength. In Fig. 2c, this case corresponds to the hogging region. Consequently, for beam BII, a brittle failure occurs over the intermediate support, while the sagging region would still have a capacity to increase the acting moment, giving rise to a load carrying capacity lower than the action assumed for design ( $q_{R,II} \leq q_E$ ). On the contrary, for beam BI, the response of the governing section is ductile, and this allows for further redistributions of internal forces, until both regions attain their resistance and the full structural capacity is reached [23]  $(q_{R,I} = q_E)$ , see Fig. 2c.

It is interesting to note thus that when brittle responses can be expected, evaluations of the internal forces deviating from the actual one can lead to unsafe designs. The consequences of this fact in terms of reliability are however not explicitly accounted for in the current Eurocodes safety format, as the safety element for the model uncertainty of action effects are only accounted for in the partial factors on actions  $(\gamma_F)$ , which is independent of the response of the structure and type of action effect analysis model. On the other side, in structures with ductile behaviour, the load carrying capacity corresponds exactly to the load assumed for design, despite the fact that the actual behaviour deviates significantly from the simplified behaviour assumed for the analysis (typically linear elastic behaviour). It can be concluded that for structures with ductile response, the model uncertainty of action effects is relatively small, whereas for brittle response, the model uncertainty of action effects shall be consistently accounted for in accordance with the type of analysis performed. This will be discussed in the following section.

# 2.2. Model uncertainty of action effects in structural concrete

The need for considering the uncertainties in calculating the internal forces in a structure, in addition to the uncertainties related to the actions, has been acknowledged already in the first attempts to quantify the partial safety factors. According to the first discussions within CEB in view of the preparation of the first Model Code [24], the partial safety factor for actions was assumed to account for the uncertainties related to calculation of the internal forces in case of refined analyses. However, for the case of typical structural analysis or in presence of particular

uncertainties, an additional partial factor  $\gamma_{Sd} = 1.12$  (1.4/1.25) increasing the value of the actions was defined [25]. This additional factor was intended to account for the uncertainties in modelling the structure, for potential errors and for neglected effects [24].

A more detailed description of the uncertainties considered with this additional partial safety factor, including an estimate of the coefficients of variation of the ratio between actual and calculated internal forces  $E_{exp}/E_{calc}$ , has been proposed in the CEB Manuals "Structural Safety" [26–28]. The considered uncertainties (coefficients of variation in brackets) were:

- (i) effect of differences between the actual structure and the idealized system assumed in the analysis (see uncertainty AE1 in Figs. 1, 8% for concrete structures and 5% for steel structures);
- (ii) approximations in the analysis (5%);
- (iii) influence of imperfections during execution on the internal forces (see uncertainty AE3 in Fig. 1; 5% for concrete structures and 2% for steel structures):
- (iv) the effect of neglected actions at ultimate limit state (as for instance imposed deformations, including thermal effects and shrinkage);
- (v) the inaccuracy in determining the influence of load combinations with the chosen safety format of partial safety factors (for the uncertainties (iv) and (v), a coefficient of variation of 8% for concrete structures and of 5% for steel structures, respectively).

In addition, also the uncertainty related to the assumed probability functions of the actions has been considered (with a value of the coefficient of variation between 0 and 5% depending on the coefficient of variation of the action). It has to be noted, that in the safety format of Fig. 1, this effect should be accounted for in the partial safety factor of the actions (see also change in the latest draft of prEN 1990:2020 [18]) so that it is not considered in the following.

The coefficient of variation of the ratio between actual and calculated action effect ( $E_{exp}/E_{calc}$ ) can be obtained from the square root of the sum of the squares. For concrete structures, the total coefficient of variation becomes  $V_{Sd}=0.125~(0.08^2+0.02^2+0.05^2+0.08^2)$  whereas for steel structures,  $V_{Sd}=0.076~(0.05^2+0.02^2+0.02^2+0.05^2)$ . In [28], the partial safety factor  $\gamma_{Sd}$  has been calculated based on reliability analysis assuming a probability of failure and a coefficient of variation for the actions. The obtained values were approximately 1.125 for concrete and 1.075 for steel structures, respectively. Similar values could be obtained following the approach of [9] by assuming lognormal distributions, a target reliability index  $\beta_{tgt,50}=3.8$  and a sensitivity factor for non-dominating actions ( $\alpha=0.4$ ) leading to  $\gamma_{Sd}=\exp(0.4\cdot0.70\cdot3.8\cdot0.125)=1.14$ .

According to the knowledge of the authors, this is the most detailed description of the uncertainties covered by the partial factor  $\gamma_{Sd}$  still available in the literature and the result has been acknowledged in different codes (current Eurocode "Basis of structural design [9] for instance, defines values of  $\gamma_{Sd}$  between 1.05 and 1.15, see Table A1.2(B), note 4). Nevertheless, it has to be noted that the considerations described above reflect the state of knowledge and the engineering practice at that time (1960s and 1970s). They were highly influenced by the concern to calculate the "actual" internal forces as accurate as possible with the tools of that time (typically hand calculations or rudimentary computer programs), but surprisingly, the difference between statically determinate or indeterminate structures hasn't been considered explicitly. In addition, as shown above, for statically indeterminate structures, a significant uncertainty can arise from the difference between the mechanical behaviour assumed for the structural analysis (typically linear elastic uncracked) and the behaviour assumed for calculating the sectional resistance (typically cracked concrete with nonlinear behaviour for concrete and steel).

#### 2.3. Definition of the random variable for model uncertainties

From the case study described above, it has been observed that the model uncertainty of action effects (local value of an internal force at a given cross section) will eventually influence the model uncertainty of the load-carrying capacity of a statically indeterminate structure. As shown in the example above, in the classical design approach of structural concrete, the models used to determine action effects and resistance are not necessarily the same. The analysis of action effect is typically determined assuming a linear response and neglecting the influence of cracking (constant uncracked stiffness) whereas, for calculation of the resistance, cracking and the nonlinear response of both concrete and steel reinforcement are considered. As previously discussed, this does not have consequences at ultimate for ductile responses, but can have implications for brittle redundant systems.

With respect to the quantification of the local resistance model uncertainty, a random variable can be defined by comparing the experimentally measured local resistance with the theoretical resistance. It shall be noted that the experimental local resistance data is usually obtained by experimental programmes on statically determinate structures, so that uncertainties related to the calculation of internal forces are not relevant. The local resistance model uncertainty is thus analysed through the following ratio:

$$\theta_{R,local} = \frac{R_{exp}}{R_{calc}} \tag{1}$$

where  $\theta_{R,local}$  is the random variable for the local resistance model uncertainty,  $R_{exp}$  is the experimental local resistance and  $R_{calc}$  is the calculated resistance.

For the action effect model uncertainty, the random variable  $\theta_E$  is defined in analogy with  $\theta_{R,local}$  as:

$$\theta_E = \frac{E_{exp}}{E_{calc}} \tag{2}$$

where  $\theta_E$  is the random variable for action effect model uncertainty,  $E_{exp}$  is the experimental action effect and  $E_{calc}$  is the calculated action effect. The definition of  $\theta_E$  in Eq. (2) has however some inconsistencies because  $E_{exp}$  and  $E_{calc}$  refer to the local level while the load-carrying capacity of a structural system (potentially redundant) is governed by its global response. Due to this reason, it is not appropriate in general to directly use the variable  $E_{exp}$  / $E_{calc}$  for a given cross section to quantify the action effect model uncertainty. Instead, the global resistance model uncertainty variable of a statically indeterminate structure can be defined as:

$$\theta_{global} = \frac{q_{exp}}{q_{calc}} \tag{3}$$

where  $\theta_{global}$  refers to the random variable for the global model uncertainty,  $q_{exp}$  to the experimentally measured load-carrying capacity of a statically indeterminate structure in terms of load factor at ultimate load bearing capacity and  $q_{calc}$  to the calculated load-carrying capacity. As shown in the previous case study, the global model uncertainty contains the model uncertainty of action effects and the model uncertainty of local resistance. The model uncertainty of action effects can then be quantified by removing the model uncertainty of local resistance from that of global resistance.

### 3. Experimental programme

To investigate the flexural response of TRC structures and to provide basic test data for investigating the action effect model uncertainty of TRC in statically indeterminate structures, an experimental programme was performed. The test series consisted of nine thin slab strips tested under three-point bending load condition. The tests were performed at the Structural Concrete Laboratory of Ecole Polytechnique Fédérale de Lausanne (Switzerland) and were performed in seven consecutive days

Table 1

Mechanical properties of the mortar (mean values and coefficients of variation CoV).

		Value	CoV
Elastic Modulus of mortar	$E_{cm}$ [GPa]	31.0	2.58 %1)
Mortar tensile strength	$f_{ctm}$ [MPa]	4.4	9.43% 1)
Mortar compressive strength	$f_{cm}$ [MPa]	128.5	10%

<sup>1)</sup> Values according to [29].

**Table 2**Mechanical property of textile reinforcement in longitudinal direction (number of tests, CoV in brackets).

Fabric		CF01	CF02(#, CoV)
Net cross section	$a_{tex}$ [mm <sup>2</sup> ]	0.85	1.70
Nominal perimeter	$U_{tex}$ [mm]	7	11
Grid spacing	$e_{tex}$ [mm]	20.0	17.0
Strength 1)	$f_{tex,m}$ [MPa]	1833	1833 (5, 7.41%)
Elastic modulus 1)	$E_{tex,m}$ [GPa]	228	228 (5, 10.9%)

<sup>1)</sup> calculated on the basis of the nominal value of the net cross section

at an average age of 301 days (to ensure constant mechanical properties).

# 3.1. Mechanical properties of the materials

The mortar mix described in [29] was used for the experimental programme, composed of nearly 40 % binder and nearly 60 % aggregate (maximum aggregate size 1.6 mm). All specimens were cast on the same day following an identical procedure and preparation of the mix.

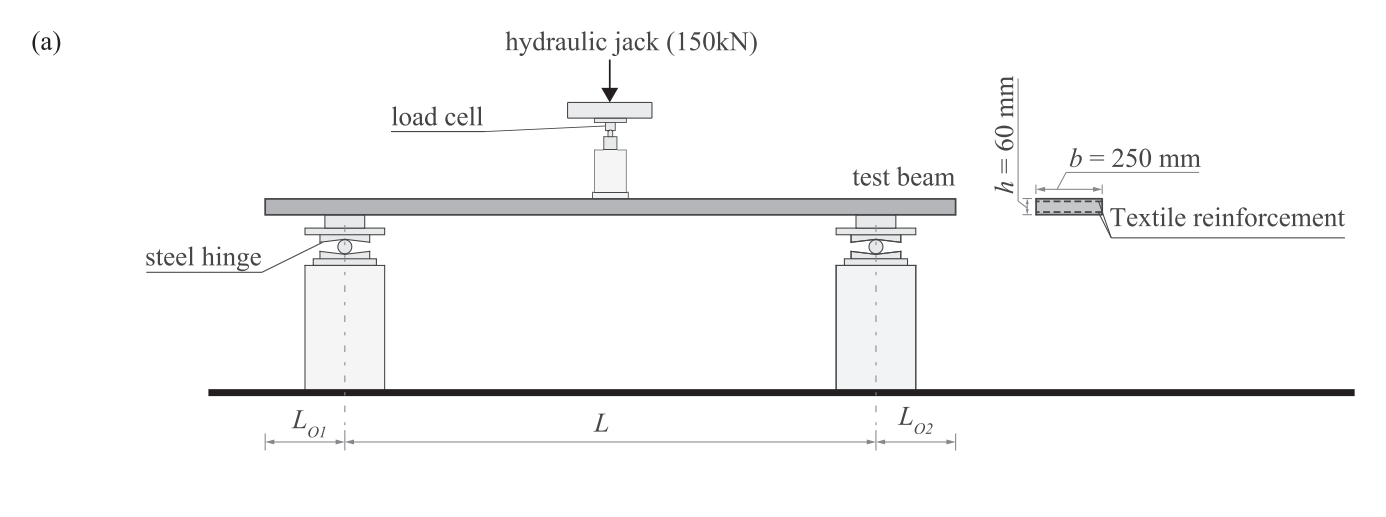
Compressive tests on the mortar produced in three batches were carried out on  $70 \times 140$  mm cylinders tested at the same period than the beam specimens. The mean value of the strength  $f_c$  of 14 compressive tests is given in Table 1. As for the elastic modulus and tensile strength of the mortar, values were derived on the basis of  $f_c$  value according to the data of [29] (results are provided in Table 1).

The textile fabrics were carbon fibre (CF) meshes. Two types of fabrics were used (named CF01 and CF02 in the following), both coated with epoxy and with a layer of quartz-sand applied to the surface, but with different net cross section area of roving (details on the geometry and main properties can be consulted in [29]). The mechanical properties of the textile fabric are given in Table 2. Bare textile (single rovings extracted from the fabric grid) were also tested in tension. Consistent with what has been observed by Valeri et al.[29], it was first observed a straightening phase of the rovings, followed by a linear response characterized by the tangent modulus of elasticity of the filament ( $E_{tex,m}$ ) until its tensile strength ( $f_{tex,m}$ ).

#### 3.2. Specimens and experimental results

The specimens had a rectangular cross section (250 mm-width and 60 mm-height) with varying span L (refer to Fig. 3 and to Table 3). All specimens were cast following the same procedure and dimensions. As the tested span length was different (Table 3), variable overhang lengths resulted ( $L_{o1}$  and  $L_{o2}$  in Fig. 3). These overhangs varied between 0.3 m and 1.2 m. Since the self-weight of the beams is relatively small compared to the failure load, the influence of the overhang length in the overall response can be considered as negligible.

The specimens were reinforced with the textiles CF01 or CF02, that were intentionally not kept with a constant cover, but only attached at



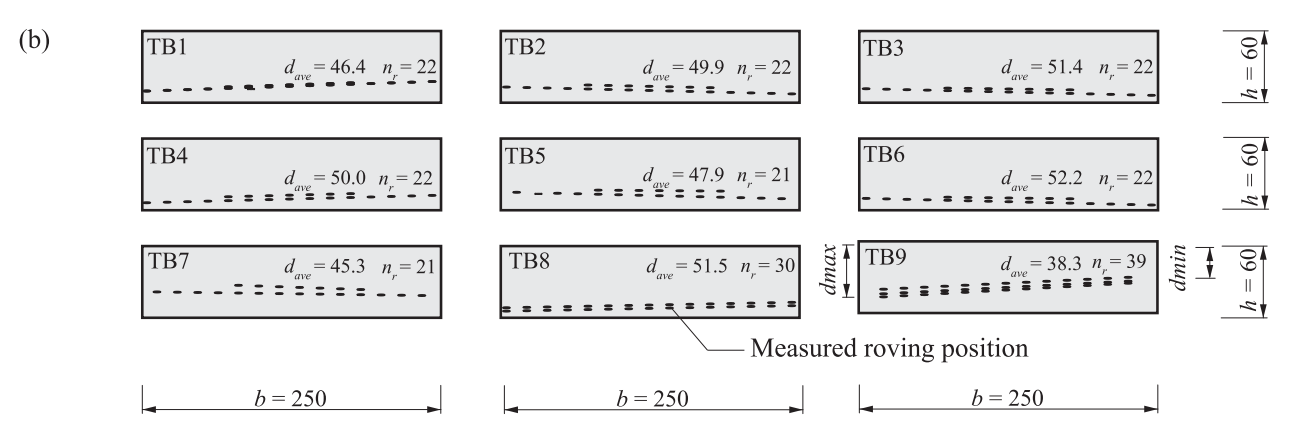


Fig. 3. Specimens: (a) test setup; and (b) representative cross section of the tested specimens (units: [mm]).

**Table 3**Main parameters of the bending specimen and measured flexural resistance at maximum load.

Name	L [m]	Textile type	Number of rovings $n_r$	$a_{tex}$ [mm <sup>2</sup> ]	$d_{min}$ [mm]	d <sub>max</sub> [mm]	d <sub>ave</sub> [mm]	$\rho_{ave}$ [%]	a/d <sub>ave</sub>	M <sub>exp</sub> [kNm]
TB1	1.2	CF02	22	1.7	42.3	50.9	46.4	0.32	12.9	2.36
TB2	1.15	CF02	22	1.7	46.4	53.8	49.9	0.30	11.0	3.33
TB3	1.1	CF02	22	1.7	49.0	55.0	51.4	0.29	11.0	3.64
TB4	2.1	CF02	22	1.7	44.5	54.7	50.0	0.31	21.5	2.77
TB5	2.2	CF02	21	1.7	44.6	52.2	47.9	0.30	23.0	2.23
TB6	2.4	CF02	22	1.7	49.8	54.8	52.2	0.29	22.0	3.04
TB7	2.4	CF02	21	1.7	38.0	49.0	45.3	0.27	25.0	1.99
TB8	2	CF02	30	1.7	48.3	54.9	51.5	0.40	19.4	3.58
TB9	0.63	CF01	39	0.85	29.9	46.3	38.3	0.35	8.2	1.63

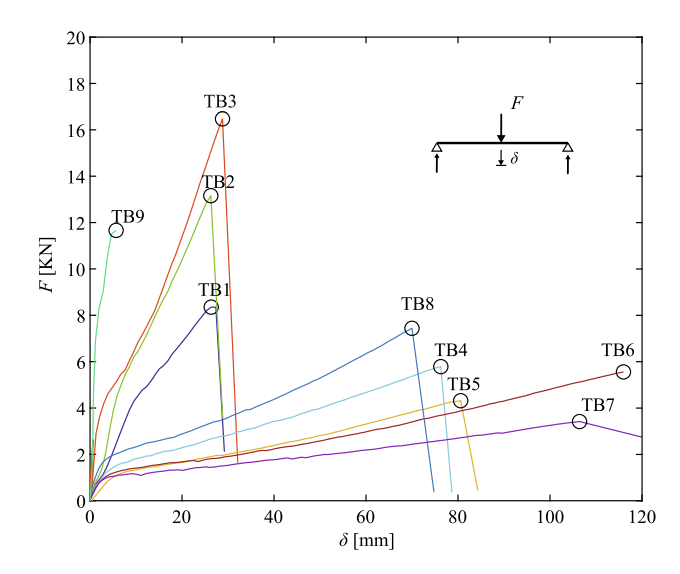


Fig. 4. Measured load-deflection responses of tested specimens.

its ends. This allowed the textile to vary its position during casting, in order to investigate the influence of construction tolerances and casting procedure in the structural response. After the bending tests were conducted, saw-cuts were performed on the specimens near the cross section failing in bending (representative cross section) and the exact position of the rovings are measured. The illustration of the measured roving positions in each cross-section is given in Fig. 3b. Since the effective depth was not constant over the beam width, the average flexural depth  $d_{ave}$  and the average flexural reinforcement ratios  $\rho_{ave}$  are defined as follows:

$$d_{ave} = \frac{\sum_{1}^{n_r} d_i}{n_r} \operatorname{and} \rho_{ave} = \frac{n_r a_{tex}}{b d_{ave}}$$
(4)

where  $n_r$  refers to the number of rovings in a cross section,  $d_i$  to the flexural depth of each roving,  $a_{tex}$  to the net cross section of a single roving and b to the cross section width. Details are given in Table 3.

Digital Image Correlation (DIC) was performed at the sides of the specimens and used to track their displacement fields following the same methodology as described in [29]. The result of DIC were checked with continuous readings obtained by means of a Linear Variable Displacement Transformers (LVDT) attached to the top side of the mid-span of each specimen. The load–deflection (F- $\delta$ ) relationships recorded for the tests are shown in Fig. 4 ( $\delta$  based on DIC measurements). For low levels of load, a linear response is observed until the cracking moment is reached. Once cracking develops, the response becomes softer, with a stiffness depending on the reinforcement ratio and slenderness. Failure occurred in all specimens in bending in a brittle manner due to rupture of reinforcement.

# 4. Bending test analysis

The flexural response of TRC can be modelled by considering a linear response of both concrete and textile reinforcement and assuming that plane sections remain plane after deformation (Bernoulli-Navier hypothesis), see Fig. 5a. This assumption has been extensively investigated and validated in previous investigations [30–36].

Due to the significant variation of the roving flexural depth in some cross sections, each roving is modelled separately for calculation of the response. Failure occurs in all cases when the outermost roving reaches its tensile strength, as it fails in a brittle manner and the rest of rovings are not capable of withstanding their increase of force. With respect to the properties of the rovings within the concrete section, their strength and stiffness have to be reduced with respect to bare textile properties (in order to account for the delayed activation of stresses and local damage [29,37–39]). This will be performed in the following by means of two distinct efficiency factors [40,41]. The first, named  $\eta_{\it f}$ , reduces the effective textile tensile strength with respect to the bare textile. The second, named  $\eta_{\it E}$ , reduces the effective modulus of elasticity of the textile.

The value of the efficiency factors is determined in this work by means of calibration with test results, in order to have an average of measured-to-calculated values equal to 1.0 both in terms of strength and deformation at failure. This yields the value  $\eta_f = 0.91$  and  $\eta_E = 0.79$ . Such approach is adopted as the aim of this paper is the statistical analysis of the TRC response (alternative approaches based on physical models to determine such efficiency factors can be consulted elsewhere [29,41]). It can be noted that the calibrated value of  $\eta_E$  is lower in this case than the value of  $\eta_f$ , which is uncommon in comparison to the results from other researchers [29,41]. This fact can be partly grounded on the fact that the roving position was variable through the length of the specimens and thus the geometry (stiffness and resistance) of the governing cross section in bending is not necessarily constant through the length of the specimen. Also, the influence of the duration of the structural tests, different to that of the material characterization tests, is accounted for in these coefficients which can be relevant for the concrete stiffness.

The calculated load–deflection curves  $(F-\delta)$  are plotted in Fig. 5c together with the measured results. The comparison between the tested ultimate resistance  $R_{exp}$ , the calculated one  $R_{calc}$  and the corresponding maximum deformation of each beam is givens in Table 4. The comparison shows that the CoV of the resistance (5.13%) is relatively low (lower than those reported by other authors [12]).

# 5. Response of statically indeterminate systems of TRC and model uncertainty of action effects

As previously explained, the response of statically indeterminate systems and the corresponding action effect model uncertainties can be significant for the safety format calibration, particularly when a brittle response can be expected. This is for instance the case for TRC, whose response was experimentally examined in the previous Section with

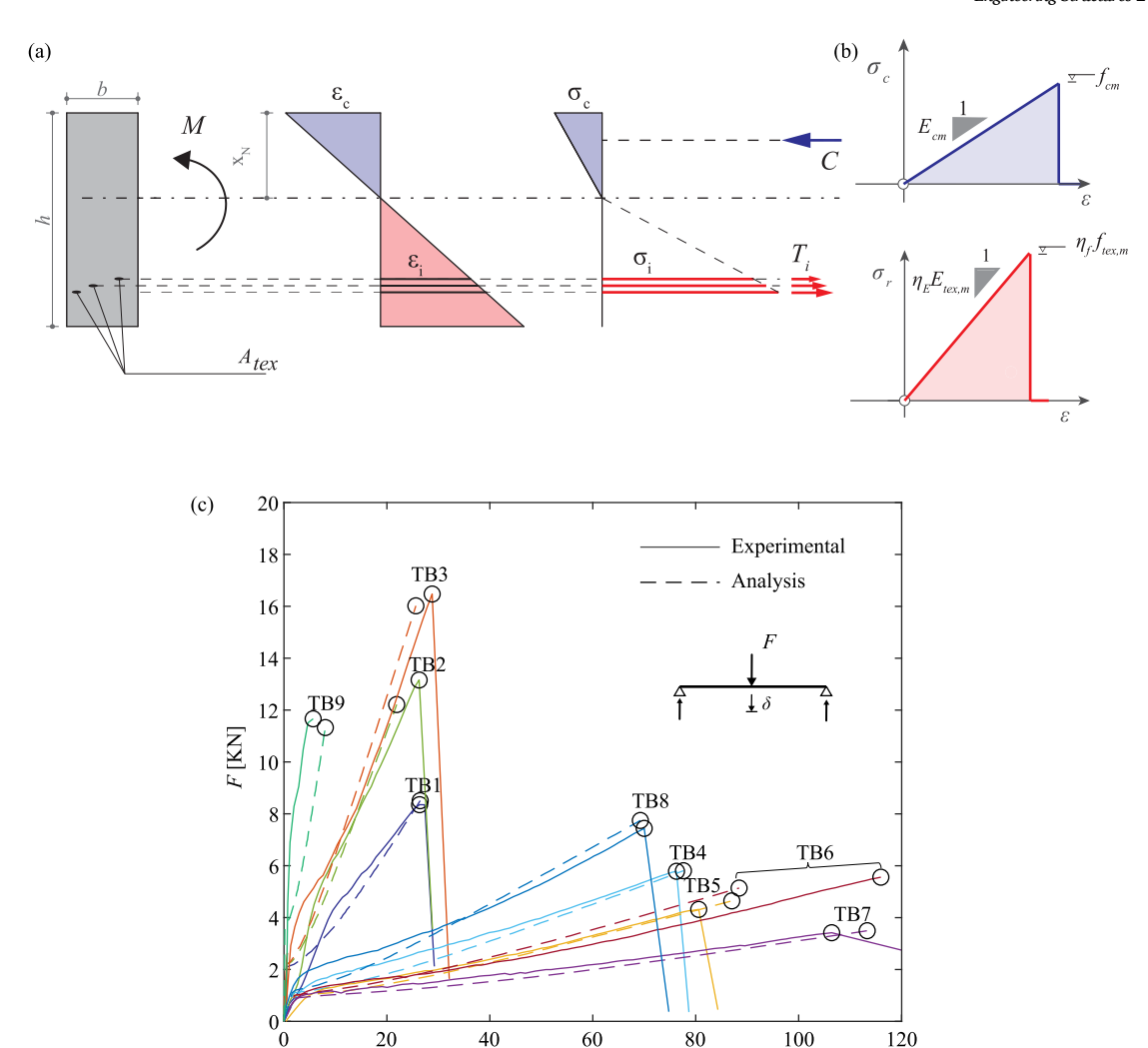


Fig. 5. (a) Model assumptions for flexural response; (b) material constitutive law of concrete and textile reinforcement and (c) calculated and experimental load–deflection curves.

 $\delta$  [mm]

Table 4
Three-point bending test results.

Specimen	R <sub>exp</sub> [kN]	R <sub>calc</sub> [kN]	$R_{exp}/$ $R_{calc}$	δ <sub>exp</sub> [mm]	δ <sub>calc</sub> [mm]	$\delta_{ m exp}/\delta_{ m calc}$
TB1	8.4	8.5	0.99	26.4	26.5	1.00
TB2	13.2	12.2	1.08	26.3	21.9	1.20
TB3	16.5	16.0	1.03	28.8	25.6	1.13
TB4	5.8	5.8	1.00	76.3	77.6	0.98
TB5	4.3	4.6	0.93	80.6	87.0	0.93
TB6	5.6	5.1	1.10	116	88.4	1.31
TB7	3.4	3.5	0.97	106.4	113.3	0.94
TB8	7.4	7.7	0.96	7.4	7.7	0.96
TB9	11.7	11.3	1.04	5.7	8.0	0.71
Average			1.0			1.0
COV			5.13%			17.10%

reference to statically determinate structures. In order to investigate the response of statically indeterminate TRC structures, it will be presented in this Section a large database obtained by assembling the test results on determinate members. This database will eventually be used to create a probabilistic model of the action effect model uncertainty.

The main idea to simulate the response of statically indeterminate members based on the response of statically determinate ones is shown in Fig. 6a (details for a worked example are provided in annex B). As it can be seen, a redundant system is generated by assembling two simply

supported beams connected at mid span. Such statically indeterminate system will be referred to in the following as an *assembled cross-beam system*. Due to the symmetry conditions of the system, each component beam has the same load–deflection response as in a three-point bending test and the response of the complete system can be obtained by the superposition of the load–deflection relationship of the two component beams, see Fig. 6b.

# 5.1. Action effect model uncertainty for different types of structural analyses

In the following, the experimental results on the assembled crossbeam systems are compared to three types of structural analyses:

- Linear Analysis assuming UnCracked stiffness (LAUC in Fig. 6b and
- Linear Analysis assuming Fully-Cracked stiffness (LAFC in Fig. 6b and c).
- NonLinear Analysis assuming uncracked and cracked behaviour.
   This analysis is conducted assuming a trilinear moment–curvature relationship and the actual extent of cracked and uncracked regions (NLA in Fig. 6b and c).

In order to quantify the model uncertainty of action effects, the local

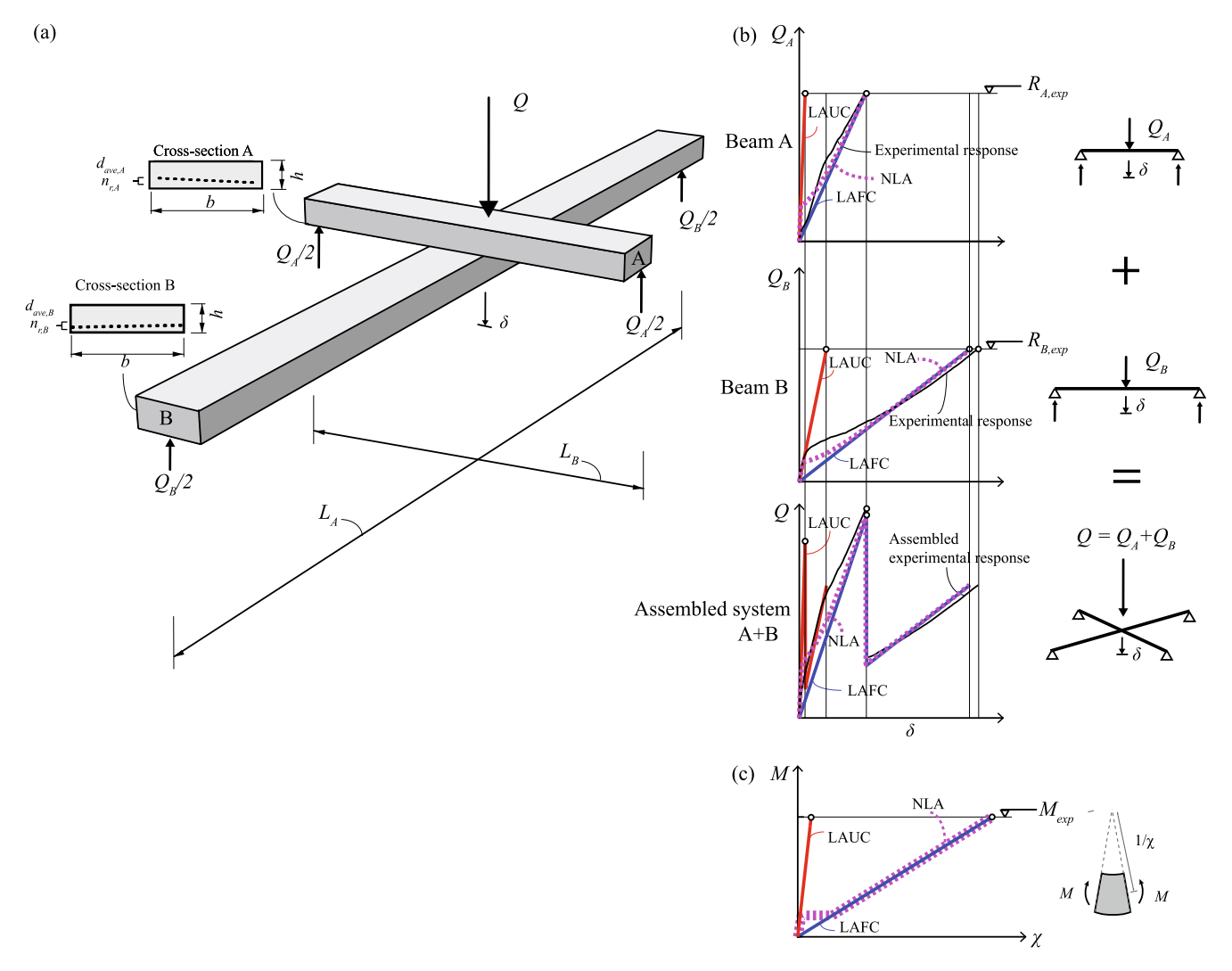


**Fig. 6.** (a) Assembled cross-beam system test set-up; (b) load–deflection relationship of the cross-beam system obtained by superposition of both responses of its component beams and (c) considered moment–curvature  $(M-\chi)$  relationships for different structural analysis models.

 $\label{eq:table 5} \textbf{Tailored efficiency factor } \eta_f \, \text{for the basic beams.}$ 

Specimen	TB1	TB2	TB3	TB4	TB5	TB6	TB7	TB8	TB9
$\eta_f$	0.90	0.98	0.94	0.91	0.85	1.00	0.88	0.87	0.95

resistance model uncertainty will be removed from the global model uncertainty. To do so, tailored values of the efficiency factor  $\eta_f$  are calibrated for each individual beam, in order to match the experimental resistance, see Table 5. The action effect model uncertainty for each analysis method can then be defined as:

$$\theta_{E,LAUC} = \frac{Q_{exp}}{Q_{LAUC}} \tag{5}$$

$$\theta_{E,LAFC} = \frac{Q_{exp}}{Q_{LAFC}} \tag{6}$$

$$\theta_{E,NLA} = \frac{Q_{exp}}{Q_{NLA}} \tag{7}$$

where  $Q_{exp}$  refers to the experimental resistance of an assembled crossbeam system by superimposing the experimental response of its two component beams. The terms  $Q_{LAUC}$ ,  $Q_{LAFC}$  and  $Q_{NLA}$  refer to the global resistances (load-carrying capacities) of the assembled cross-beam

system calculated with LAUC, LAFC and NLA methods respectively and  $\theta_{E,LAUC}$ ,  $\theta_{E,LAFC}$  and  $\theta_{E,NLA}$  refer to the corresponding action effect model uncertainty variables for the three types of analysis.

# 5.2. Data of action effect model uncertainty for different types of structural analyses

By combining the nine bending tests of basic beams presented in Section 3, a total of 36 assembled cross-beam systems can be generated. The resulting action effect model uncertainty data is plotted in Fig. 8a. The assembled experimental load–deflection curves of six representative cases and the corresponding load-deformation curves with LAUC, LAFC and NLA are shown in Fig. 7. A summary of the results of all the assembled cross-beam tests is also provided in Table 6 and plotted in Fig. 8a. As it can be noted, both NLA and LAFC give very close prediction to the actual resistance, while LAUC has a relatively larger scatter, suggesting that the simplifications made about the uncracked stiffness of the structure components result in a higher model uncertainty for

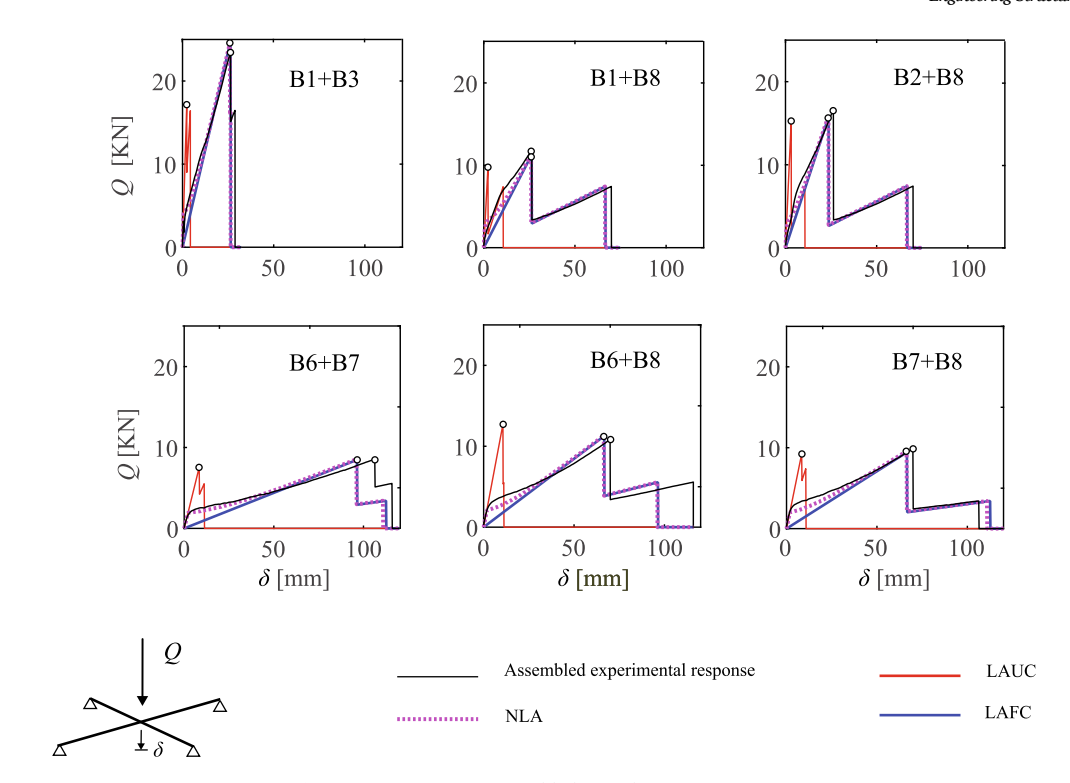


Fig. 7. Representative assembled cross-beam system cases.

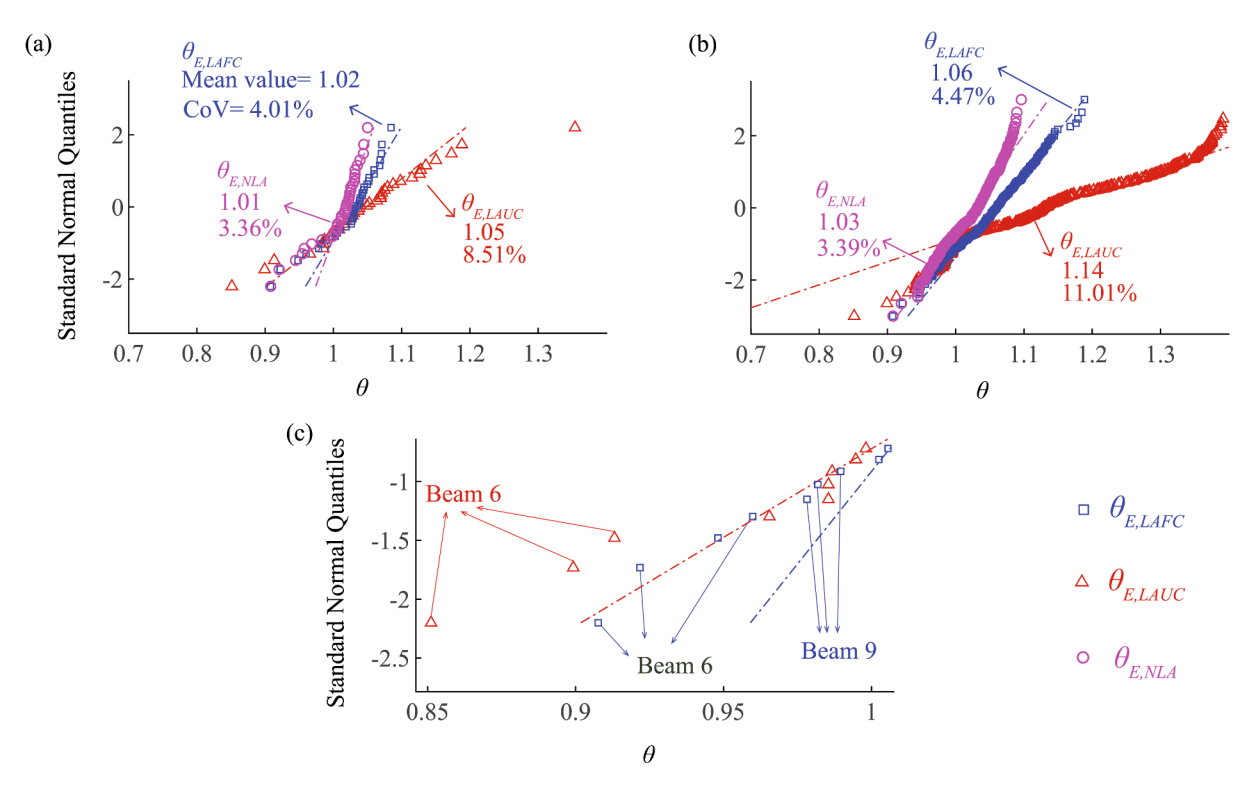


Fig. 8. Quantile-Quantile plot for action effect model uncertainty sample data of (a) cross-beam of two components; (b) cross-beam of two to five components; and (c) detail of tail region for cross-beam of two components.

statically indeterminate structures. In addition, NLA allows reproducing the different stages of response (uncracked or partially cracked) in a realistic manner.

To further increase the size of sample for action effect model uncertainty data, the number of components of a cross-beam system can still be increased in order to generate more combinations. Following the

same methodology, assembled cross-beam system composed of three to five components are further investigated. In total, 372 different cross-beam systems are generated and the resulting action effect model uncertainty data is plotted in Fig. 8b. A summary of the statistics of the assemble cross-beam tests is provided in Table 6. It can be observed that, with the enlarged database, the difference between the model

Table 6
Statistics of the cross-beam system tests with two components and two to five components.

Number of components	Number of assembled tests	Load effect analysis	Variable	Average value	CoV
Two	36	LAUC	$\theta_{E,LAUC}$	1.05	8.51%
	36	LAFC	$\theta_{E,LAFC}$	1.02	4.01%
	36	NLA	$\theta_{NLA}$	1.01	3.35%
Two to five	372	LAUC	$\theta_{E,LAUC}$	1.14	11.01%
	372	LAFC	$\theta_{E,LAFC}$	1.06	4.47%
	372	NLA	$\theta_{NLA}$	1.03	3.39%

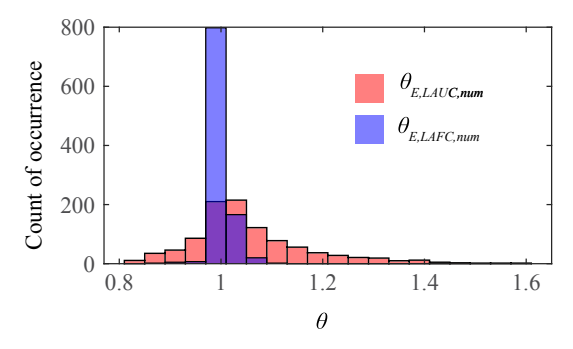


Fig. 9. Histogram of the  $\theta_{E,LAUC,num}$  and  $\theta_{E,LAFC,num}$  data from the numerical assembled cross-beam system case study.

**Table 7**Statistics of the numerical cross-beam system tests with two components.

Number of fictitious tests	Load effect analysis	Variable	Average value	COV
1000	LAUC	$\theta_{E,LAUC,num}$	1.06	11.21%
1000	LAFC	$\theta_{E,LAFC,num}$	1.00	1.66%

uncertainty data of the NLA, LAUC and the LAFC method is more pronounced, which confirms that the NLA and LAFC result in lower level of action effect model uncertainty than the LAUC.

As shown in Fig. 1, the action effect model uncertainty of statically indeterminate system results from multiple sources as: the uncertainties related to the structural modelling of action effects; the uncertainties in material properties influencing action effects; and the uncertainties in geometrical properties influencing action effects. The result shows that NLA yields to the lowest CoV level, which signifies that NLA can significantly reduce the uncertainties related to the structural modelling of action effect. Comparing the tail region of NLA, LAUC and LAFC from the Quantile-Quantile plot [42] (vertical axis referring to quantiles in a standard normal distribution) of  $\theta_{E,NLA}$ ,  $\theta_{E,LAFC}$  and  $\theta_{E,LAUC}$  data (see Fig. 8a) it seems however that in the tail region there is no significant difference between these three distributions. This is explained by the fact that the tail region is composed only of results concerning two beams (specimens 6 and 9) influencing the response of all methods to evaluate the internal forces, see Fig. 8c.

# 6. Limits of applicability of linear analyses assuming uncracked and fully-cracked behaviour

The analyses on statically indeterminate structures based on the assembled cross-beams are based on the three-point bending tests data tested within this research program. This implies that only a limited range of the basic design variables has been explored. In this Section, the applicability of LAUC and LAFC will be investigated for a wider range of design cases.

To that aim, the same methodology of the assembled cross-beam system is used in this section. The basic data for the three-point bending test is in this case estimated on the basis of a non-linear analysis (tri-linear moment–curvature relationship). This approach was previously observed to lead to the most realistic results, and to reproduce the various regimes of response (see Fig. 7). A series of numerical assembled cross-beam system case studies are generated by varying the span L, the cross-section height h, and the textile reinforcement cross-section area  $A_{tex}$  of the component beams. By comparing the structural analysis result (global resistance of the structures) from the LAUC and the LAFC with that of NLA, the limit of applicability of LAUC and LAFC is further examined.

# 6.1. Range of design parameters of numerical case study

In the numerical cases, assembled cross-beam systems with two component beams with rectangular cross-sections (refer to Fig. 6) are studied. In order to investigate the influence of the variation of relative stiffness between the component beams, the dimensions of the first component beam in the assemble cross-beam system is kept constant and the dimensions of the second beam are varied in the selected range.

For all the component beams of the assembled cross-beam systems, the cross-sectional width is kept constant (b=250 mm). The material parameters are also kept constant, adopting the same material properties as for Section 3. To simplify the simulation, all textile reinforcements in a given beam are considered to be aligned at the same depth. Three independent parameters are used to characterize the beams in the numerical cases: the span L, the cross-section height h, and the textile reinforcement cross section area  $A_{tex}$ . The vector composed of the three design parameters form the design vector  $X_{num}$  for a given component beam:

$$X_{num} = [L, h, A_{tex}] \tag{8}$$

For a given component beam, the other parameters are dependent on the values of its design vector  $X_{num}$ : the cross-sectional effective depth of a given component beam (d) is assumed to be proportional to the height h with a constant ratio d=0.85~h and the reinforcement ratio  $\rho$  is defined as  $\rho=\frac{A_{tot}}{h_{tot}}$ .

In each numerical case, two beams are assembled. The design vector of component beam A is always kept constant as  $X_{num,A} = [L_A, h_A, A_{tex,A}]$ , with  $L_A = 1.7$  m,  $h_A = 60$  mm and  $A_{tex} = 66.3$  mm² (resulting in  $\rho_A = 0.52\%$ ). The design vector of component beam B (denoted by  $X_{num,B,ijk}$  with i,j,k=1-10) is varied. The design parameters of beam B are varied within the following range:  $L_{B,i} = (1.0-4.0)$  m;  $h_{B,j} = (30-120)$  mm and  $A_{tex,B,k} = (23.8-142.8)$  mm², resulting in  $\rho_{B,ijk} = (0.09-2.24)\%$  (i,j,k=1-10). For each parameter, ten equally spaced values in the ranges specified are considered, leading to a total of 1000 cases. For example, for the case of [i,j,k] = [1,1,10],  $X_{num,B,ijk} = [L_{B,1},h_{B,1},A_{tex,B,10}]$ , with  $L_{B,1} = 1.0$  m,  $h_{B,1} = 30$  mm and  $A_{tex,B,10} = 142.8$  mm² (resulting in  $\rho_B = 2.24\%$ ).

For each case, the resistance of the assembled cross-beam system analysed with LAUC and LAFC (refer to Annex B for the detailed analysis method) are compared with that analysed with NLA in order to get the corresponding action effect model uncertainty data:

$$\theta_{E,LAUC,num} = \frac{Q_{NLA}}{Q_{LAUC}} \tag{9}$$

$$\theta_{E,LAFC,num} = \frac{Q_{NLA}}{Q_{LAFC}} \tag{10}$$

It should be noted that  $\theta_{E,LAUC,num}$  and  $\theta_{E,LAFC,num}$  only contains uncertainties related to the structural modelling of action effects and are thus different than the definition of  $\theta_{E,LAUC}$  and  $\theta_{E,LAFC}$  in the previous section (Section 5.1 Eqs. (5)–(6)).

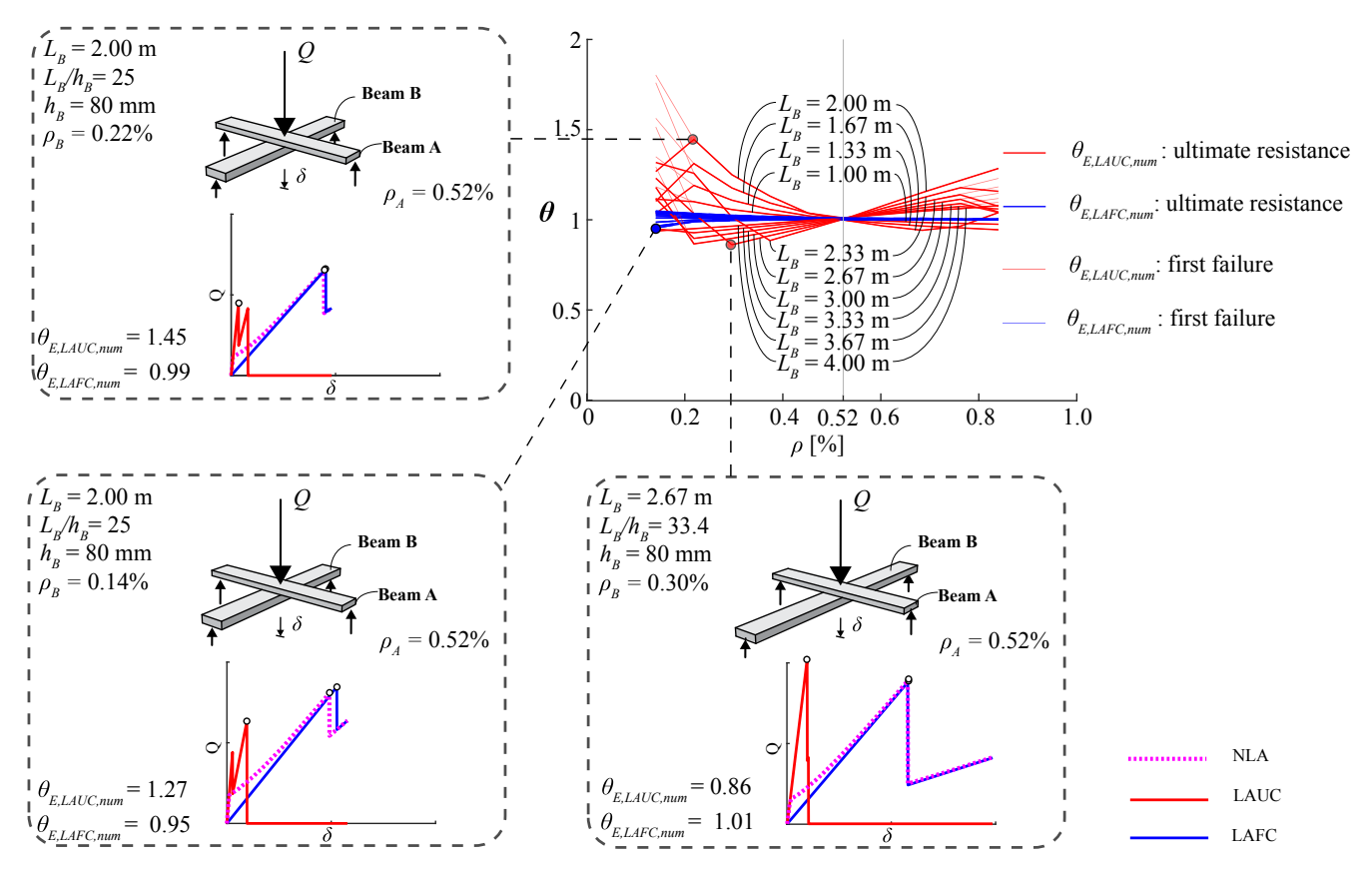


Fig. 10. Results of  $\theta_{E,LAUC,num}$  and  $\theta_{E,LAFC,num}$  for cases with  $h_B=80$  mm.

**Table 8**Probabilistic modelling of basic random variables for safety format calibration of TRC.

Uncertainty type	Variable	Distribution	Mean Value	CoV	Standard deviation
Material	Textile reinforcement tensile strength $f_{tex}$	Lognormal [43]	$f_{tex,m}$	15% [29]	-
	Concrete compressive strength $f_c$	Lognormal [43]	$\eta_{is}f_{cm}$	15.6% [18]	-
Geometrical	Flexural depth d	Normal [43]	$d_{nom}$	-	3 [mm] [12]
Model	Resistance model uncertainty $\theta_{R,local}$	Lognormal [43]	1.0	10% [12]	0.1

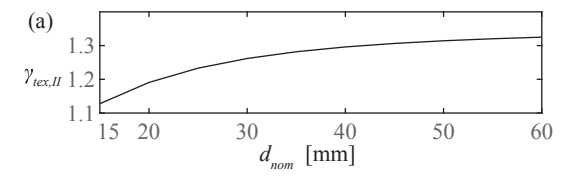
# 6.2. Results of the case study

The histograms of the resulting  $\theta_{E,LAUC,num}$  and  $\theta_{E,LAFC,num}$  data for all cases are plotted in Fig. 9 and the statistical values are given in Table 7. It can be observed that, in general, the LAFC results in smaller scatter in the action effect model uncertainty.

To have a better understanding of the limit of applicability of the two methods, the resulting  $\theta_{E,LAUC,num}$  and  $\theta_{E,LAFC,num}$  for the cases with  $h_B=$ 

80 mm are plotted in Fig. 10. As it can be seen in this figure,  $\theta_{E,LAUC,num}$ has significantly higher variation than  $\theta_{E.LAFC.num}$ . For the cases when the reinforcement ratio of both beams is similar, the LAUC method yields a  $\theta_{E,LAUC,num}$  value close to 1, but in a wide range of cases the value of  $\theta_{E,LAUC,num}$ LAUC, num deviates significantly from 1. On the other hand, the LAFC yields in most cases  $\theta_{E,LAFC,num}$  values close to 1. This confirms the applicability of the LAFC method in general. The result of the LAFC only deviates significantly from the expected value when the reinforcement ratio of Beam B is close to the minimum reinforcement ratio for bending. This means that a significant portion of the beam remains uncracked at failure and thus, the fully cracked assumption deviates from the actual response. For practical purposes, this situation can be avoided by requiring a reinforcement ratio higher than the minimum. It is also interesting to notice that in the cases where the two component beams have the same reinforcement ratio ( $\rho_B = \rho_A = 0.52\%$ ), despite the variation of other parameters, the result  $\theta_{E,LAUC,num}$  and  $\theta_{E,LAFC,num}$ values remain close to 1. This is because the ratio between the uncracked stiffness of the two beams are the same as the ratio between their fully cracked stiffness in these cases.

As a conclusion from the previous considerations, it can be observed that, unlike for ordinary reinforced concrete structures, it is not advised to use the LAUC method to perform action effect analysis for TRC structures. A LAFC can, on the other hand, be applied provided that sufficient amount of flexural reinforcement is provided. It should also be



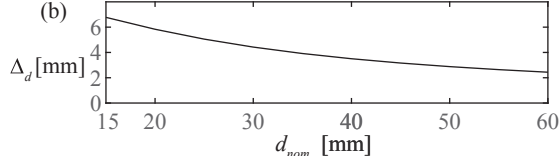


Fig. 11. Estimated values as a function of nominal effective depth: (a)  $\gamma_{tex,II}$ ; and (b) $\Delta_d$ .

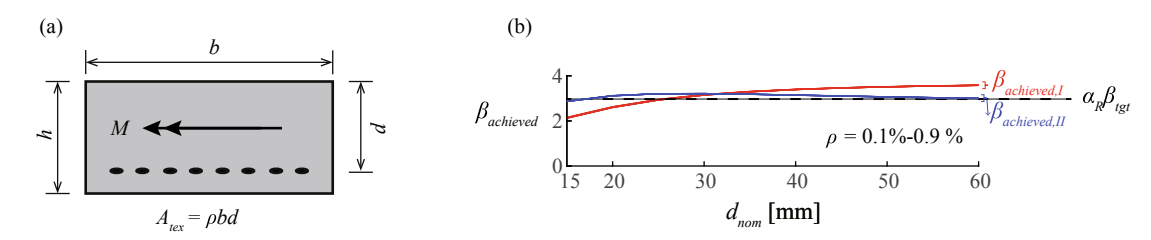


Fig. 12. (a) Geometry of the investigated cross section and (b) achieved reliability index of the investigated bending case with the two safety format proposals.

**Table 9**Key design parameters for the representative cases.

Variable	f <sub>tex,m</sub> [MPa]	f <sub>cm</sub> [MPa]	b [mm]	h [mm]	d <sub>nom</sub> [mm]	ρ
Value	1800	150	250	18.75–75	0.8 <i>h</i>	0.1% – 0.9%
Variable type	Random variable	Random variable	Deterministic	Deterministic	Random variable	Deterministic

noted that the previous comments focus on the cases with bending failure governed by rupture of the textile reinforcement (covering also cases with low levels of axial compression forces). Other failure modes (such as failures for very high levels of compression forces or shear) remain outside of the scope of this paper (covered by other partial safety factors).

#### 7. Safety format of TRC structures

In this section, the reliability verification framework of Eurocodes [9] is used to calibrate the safety format for TRC structures on the basis of probabilistic reliability theory. Similar to the case of reinforced concrete structures, a number of uncertainties (associated to material, geometry and modelling) shall be accounted for in the partial factor for TRC. In addition, due to the brittle behaviour of TRC structures, it is necessary to discuss if additional safety considerations are needed for the model uncertainty of action effects (a common situation with respect to design of other reinforced concrete elements failing in a brittle manner by punching or second-order effects). In the following, the probabilistic modelling of the basic uncertainties is discussed and two types of safety formats are proposed for TRC structures. The efficiency of the proposed safety formats for TRC structures is discussed based on the reliability analysis of representative cases.

# 7.1. Basic uncertainties in the design of TRC structures

# 7.1.1. Material uncertainties

Two material strength basic variables are involved in the reliability analysis problem of TRC structures: the tensile strength of textile reinforcement and the concrete compressive strength. The material strength variables are assumed to follow lognormal distribution according to the recommendations in [43]. For the concrete compressive strength, the distribution parameters provided in the second generation of Eurocode prEN1992-1-1:2020 [44] are used, where the coefficient of variation (CoV) is taken as 15.6%, which accounts for both the uncertainty in concrete cylinder strength and the uncertainty in the in-situ strength efficient factor  $\eta_{is}$  [44]. For the distribution parameters of the textile reinforcement tensile strength, the statistics of the data from [29] are used, where the CoV of the tensile strength of textile reinforcement is taken as 15% (which accounts for the uncertainty in the single roving tensile strength based on test results). These distribution parameters are consistent with data from other researchers [12]. The uncertainty in the efficiency factor  $\eta_f$  of textile reinforcement is not accounted for in the material uncertainty, but in the uncertainty of the resistance model (calibration factor). It should be emphasized that with respect to the statistical properties for the textile reinforcement tensile strength, they should be based on the data provided by the manufacturer or derived

from specific tests (products can have highly variable properties). The probabilistic modelling of the material strength variables used in the safety format calibration in this paper is summarized in Table 8.

#### 7.1.2. Geometric uncertainties

Since the case of bending is considered and the material strength of textile reinforcement is calculated on the basis of the nominal value of the roving area, the governing geometrical value is the effective geometrical depth (d). Its uncertainties are mainly related to how the reinforcement is fixed during casting, to the type of the member (with flanged or full cross section), to the casting and control procedure and to the type of reinforcement (stiff or soft). Statistical data of the flexural depth variable can be found in literature. According to [12], a mean value of -0.2 mm and a standard deviation of 2.0 mm of the measured data is observed for the deviation (error) of the flexural depth from nominal values (d- $d_{nom}$ ). This shows that it is possible to have relatively good quality control of the position of the textile reinforcement in TRC structures. For practical applications of TRC structures, the distribution parameters of the flexural depth random variable will be considered related to their quality control and allowable execution tolerance. Since the total thickness of TRC structures is in general much smaller than in ordinary concrete structures, the assumptions of execution tolerances of concrete structures are not considered applicable to TRC structures. Referring to the data from [12] and also taking the efficiency of the textile reinforcement into account, a tolerance of  $\pm -5$  mm for the error of effective depth  $(d-d_{nom})$  will be assumed in the following. The error of effective depth  $(d-d_{nom})$  is assumed to follow a normal distribution, with a mean value of 0, and -5 mm corresponds to the 5% fractile. Based on the normal distribution assumption, the standard deviation of d- $d_{nom}$  can then be calculated as 5/1.645 = 3.0 mm. Since  $d_{nom}$  is a deterministic value, the flexural depth variable d has the same standard deviation (3 mm) as d- $d_{nom}$ , see Table 8. It should be noted that, with a constant value of execution tolerance for the flexural depth, the CoV of the flexural depth variable decreases with the increasing thickness of the structure. The same phenomenon has also been noticed in reinforced concrete structures in the second generation of Eurocode prEN1992-1-1:2020 [44].

# 7.1.3. Model uncertainties

Two types of model uncertainties are considered for the partial factor calibration of TRC structures: (i) the resistance model uncertainty and (ii) the action effect model uncertainty. For the resistance model uncertainty variable,  $\theta_{R,local}$ , the model used to analyse the tests presented in this paper showed a fairly low CoV (equal to 5.13%). Such low value results partly from the fact that a calibrated value of the efficiency factor  $\eta_f$  was adopted. When designing TRC structures, a general value of this efficiency factor shall be adopted (not calibrated based on tests),

potentially leading to a higher value of CoV of the model uncertainty variable. Based on the work of other researchers [12,13,16], a reasonable value for the CoV can be considered as 10%, that will also be used in the following, see Table 8.

For the action effect model uncertainty, as previously explained in Fig. 1, it is theoretically accounted for in the partial factors for the actions provided in Eurocodes. It shall yet be noted that the model uncertainty of action effects accounted for by these partial factors depend neither on the material response (brittle or ductile) nor on the structural analysis methods (LAUC, LAFC, NLA or others). For TRC structures, it has been shown in this paper that when using NLA or LAFC for a redundant structure, the model uncertainty of action effects is relatively low compared to the values reported in Section 2.2 and to other uncertainties reported in Table 8 (maximum CoV = 4.47% for the investigated cases). This is however not the case for LAUC (maximum CoV = 11.01%). Based on this consideration, it is proposed that both NLA and LAFC methods can be used to calculate the action effect (internal forces) of TRC structures without the need to adjust the action effect model uncertainty level. LAUC cannot however be used, unless additional specific considerations were made on the safety factors.

# 7.2. Safety format proposals

Based on the characteristic of basic uncertainties involved in the resistance of TRC structures, two types of safety formats are proposed.

7.2.1. Safety format I: Partial factor  $\gamma_{tex,I}$  for the tensile strength of textile reinforcement and consideration of nominal dimensions

The first proposal for the safety format is based on the use of a partial factor for the strength of the textile and the use of nominal values for the geometric dimensions. This approach corresponds thus to current design practice for conventional reinforced concrete structures, but providing a tailored partial safety factor for the strength of the reinforcement.

The calculation of the value of the partial safety factor can be performed assuming that the resistance function R can be approximated by a lognormal distribution (detailed information about such an estimation is provided in Annex A). Thus, the partial safety factor  $\gamma_{tex,I}$  for calculation of the design value of the tensile strength of textile reinforcement ( $f_{tex,d} = f_{tex,ck}/\gamma_{tex,I}$ ) can be calculated based on the approximated value of the CoV of the resistance,  $V_R$ :

$$\gamma_{tex,I} = \frac{f_{tex,ck}}{f_{tex,d}} = \exp(\alpha_R \beta_{tgt} V_R - 1.645 V_{ftex})$$
(11)

Where  $f_{tex,d}$  refers to the design value of the textile tensile strength,  $f_{tex,ck}$  to its characteristic (5% fractile) value,  $\alpha_R$  to the FORM sensitivity factor for the resistance (adopted equal to 0.8 [9]),  $\beta_{tgt}$  to the target reliability index and  $\beta_{tgt} = 3.8$  for structures with medium consequence class and a reference period of 50 years at the ultimate limit state [9],  $V_R$  to the CoV of the resistance variable and  $V_{ftex}$  the CoV of the material (15% according to Table 8). With respect to  $V_R$ , its value can be approximately estimated (detailed information about such an estimation is provided in Annex A) by considering the CoVs for the material, geometrical and model uncertainties (refer to Table 8) as:

$$V_R \approx \sqrt{V_{\theta_R}^2 + V_{flex}^2 + V_d^2} \tag{12}$$

The general format to calculate the design value of the resistance ( $R_d$ ) can thus be established as:

$$R_d = R\left\{\frac{f_{lex,ck}}{\gamma_{lex,l}}, \frac{f_{ck}}{\gamma_C}, d_{nom}\right\}$$
 (13)

Where  $f_{ck}$  refers to the characteristic compressive strength of concrete,  $\gamma_C$  to its partial safety factor (1.5 according to Eurocode prEN1992-1-1:2020 [44]) and  $d_{nom}$  to the nominal value of the geometrical

dimensions.

Detailed information about the safety format calibration method is provided in Annex A. As it can be noted, the estimated value of  $V_R$  varies with the change of the nominal effective depth of the structure (see Table 8). For the investigated range of the nominal effective depth (15–60 mm), the estimated value of  $V_R$  ranges between 0.19 and 0.27 (see detailed results in Annex A). It should be noted that according to prEN1990:2020 [18], when  $V_R$  is higher than 0.20, the approximated Eq. (11) is not applicable for the partial factor calibration anymore. In this section, however, Eq. (11) is still used to make a first approximated calculation of the partial safety factor. Its effectiveness will be verified by the reliability case study in Section 7.3. Considering the wide applicable range of the safety format, referring to the approximated estimation values of  $V_R$ , a relatively conservative value of  $V_R = 0.225$  is selected in the following and the value of the partial factor  $\gamma_{tex,I}$  is then calculated as:

$$\gamma_{tex,I} \approx 1.55$$
 (14)

It should be noted that the partial factor for concrete compressive strength  $\gamma_C=1.5$  from Eurocode prEN1992-1-1:2020 [44] is also adopted in this research. The effectiveness of this proposal will be verified in Section 7.3 by calculating the actual achieved reliability level of representative cases.

7.2.2. Safety format II: Partial factor  $\gamma_{tex,II}$  for the tensile strength of textile reinforcement and consideration of design values for the dimensions

As shown in Annex A, for thin members, the geometrical uncertainties (related to the effective depth) can become governing. For this reason, it makes sense to separate the geometrical uncertainties from material and model uncertainties as previously discussed by [12,13]. Considering the general form of the limit state function and the probabilistic models of the basic uncertainties (see details in Annex A), the material and model uncertainties will be lumped into one partial factor  $\gamma_{tex,II}$  applied to the tensile strength of textile reinforcement. With respect to the geometrical uncertainties, they will however be considered apart, by means of a design value of the effective depth (this alternative possibility using design values of geometrical dimensions is already given by prEN1992-1-1:2020 [44]). The partial safety factor can thus be estimated with the help of FORM sensitivity factors as:

$$\gamma_{tex,II} = \frac{f_{tex,ck}}{f_{tex,d}} = \exp\left(\sqrt{\alpha_{flex}^2 + \alpha_{\theta}^2} \sqrt{V_{flex}^2 + V_{\theta}^2} \alpha_R \beta_{tgt} - 1.645 V_{flex}\right)$$
(15)

Details on this derivation and the values for the various parameters are given in Annex A of this paper. With respect to the design value of the effective depth, it is calculated by reducing the nominal value by a distance of  $\Delta_d$ :

$$d_{design} = d_{nom} - \Delta_d \tag{16}$$

whose value results (see Annex A for details):

$$\Delta_d = \alpha_d \alpha_R \beta_{tgt} \sigma_d \tag{17}$$

Based on the safety elements defined above, the general format to calculate the design value of resistance can be defined:

$$R_d = R\left\{\frac{f_{tex,ck}}{\gamma_{tex,II}}, \frac{f_{c,ck}}{\gamma_C}, d_{design}\right\}$$
(18)

By applying this methodology, the value of the partial factor  $\gamma_{tex,II}$  and  $\Delta_d$  can be derived for the given range of  $d_{nom}$ , as shown in Fig. 11 for representative cases.

It can be observed that the estimated value of  $\gamma_{tex,II}$  ranges between 1.13 and 1.33 and the value of  $\Delta_d$  between 6.8 mm and 2.4 mm. As a reasonable and safe estimate, the following values are suggested:

$$\gamma_{tex,II} \approx 1.25 \tag{19}$$

$$\Delta_d \approx 6mm$$
 (20)

The effectiveness of this proposal will be verified and compared with Proposal I in Section 7.3 by calculating the actual achieved reliability level of representative cases.

#### 7.3. Comparison and verification of the two safety format proposals

A series of representative cases are investigated in the following to compare the previous proposals. To that aim, the classical design method of verifying at sectional level is considered, implying that the influence of statically indeterminate structures is taken into account by the partial factor on actions. The geometry of the studied cross section is shown in Fig. 12a. The range of the key design parameters used in this case study series is listed in Table 9. The value of cross-section height h and reinforcement ratio  $\rho$  are varied in a deterministic manner to generate a series of different cases.

For the reliability analysis, the basic uncertainties introduced in Section 7.1 (listed in Table 8) are accounted for. The general form of the performance function *g* is defined as:

$$g = \theta_{R,local} R(f_{tex}, f_c, d) - R_d$$
 (21)

Based on the safety format proposals, the design value of the resistance for the two safety formats can be calculated using Eq. (13) and Eq. (18) and the reliability analysis is performed using FORM to calculate the actual achieved reliability  $\beta_{achieved}$  for the two types of safety formats as:

$$Prob(g < 0) = \Phi(-\beta_{achieved}) \tag{22}$$

Where Prob () refers to the probability function, g to the performance function,  $\Phi$  to the cumulative probability function of standardized normal distribution and  $\beta_{achieved}$  refers to the actual achieved reliability index for a given case. The reliability analysis is performed with FORM method and the achieved reliability index from the two safety proposals are plotted in Fig. 12b.

As it can be observed, the value of the achieved reliability level for Proposal I,  $\beta_{achieved,I}$ , ranges between 2.12 and 3.66 and the value of the value of the achieved reliability level for Proposal II,  $\beta_{achieved,II}$ , ranges between 2.87 and 3.22. Comparing the achieved reliability index for the two proposals with the target of  $\alpha_R\beta_{lgt}=3.04$ , it can be observed that in most of the range of the investigated cases, both safety formats result in acceptable levels of reliability. However, for Proposal I, when the effective depth is very low (smaller than 20 mm), the achieved reliability level is lower than the acceptable level ( $\pm 0.5$  target level) [21]. It can also be observed that the maximum achieved reliability level for Proposal I is even high for large thicknesses, suggesting potentially uneconomic design. Proposal II yields a more uniform level of reliability.

# 8. Conclusions

This paper investigates on a suitable safety format and analysis method for Textile Reinforced Concrete (TRC) structures. The results of an experimental programme on nine TRC slabs are presented and the implications of a brittle response on the reliability of a structure are discussed. Its main conclusions are listed below

1. Structures presenting brittle responses (implying limited or none redistribution capacity of internal forces) can fail for load levels below those considered for design if the calculation of internal forces deviates from the actual response (typically, elastic-uncracked behaviour assumed in the calculation of internal forces). This situation does not occur for a ductile response and raises questions on the consideration of model uncertainty of action effects within the Partial Safety Factor Format (PSFF) as considered in Eurocodes.

- 2. The analysis of statically indeterminate TRC structures shows that performing a linear elastic calculation of internal forces considering fully cracked stiffness properties for all sections is a suitable manner to estimate the internal forces and response of TRC. This holds true provided that more than minimum amount of reinforcement are provided in the structure.
- 3. Alternatively, using a nonlinear analysis (considering the development and extent of cracking) is also a suitable manner to estimate the internal forces. It is even more accurate than the previous, but requiring a significant effort for analysis.
- 4. Estimating internal forces on the basis of the uncracked stiffness of the sections (as usually performed for ordinary reinforced concrete) can lead to relatively large deviations on the response and internal forces of a brittle structure as TRC. Such method shall not be used for design unless specific considerations were implemented to cover this increased uncertainty.
- 5. Since for thin members, the variability of the effective depth can be significant compared to the mean value, the geometrical uncertainties can play a major role in calibrating the partial safety factors for designing structures at ultimate limit state. On the basis of reliable internal forces (determined by a linear-elastic fully cracked analysis or a nonlinear analysis), a safety format can be considered for TRC following the PSFF. Two ways for so doing are detailed in the manuscript:
  - o Consideration of a partial safety factor for the tensile strength of the textile ( $\gamma_{tex}=1.55$ ) and nominal dimensions. All uncertainties (material, geometrical and model) are lumped into the partial safety factor of the textile.
  - o Consideration of a reduced partial safety factor for the tensile strength of the textile ( $\gamma_{tex}=1.25$  and design dimensions (reduction of 6 mm in effective depth). In this case, material and model uncertainties are accounted for in the partial safety factor of the textile while geometrical uncertainties are considered in the design dimensions.
  - o In general, the second safety format is preferable, leading to a more uniform level of safety.

It shall be noted that the aim of this investigation is to propose a safety format for designing TRC and a methodology for calibrating the associated safety factors and parameters. For practical applications, the values proposed in this investigation ( $\gamma_{tex}$  and  $\Delta_d$ ) should be tailored on the basis of actual values of material and geometrical uncertainties, which can depend on the material used, production method and quality control procedure.

# CRediT authorship contribution statement

Qianhui Yu: Conceptualization, Methodology, Validation, Formal analysis, Investigation, Resources, Data curation, Writing – original draft, Writing – review & editing. Patrick Valeri: Conceptualization, Formal analysis, Writing – review & editing, Project administration. Miguel Fernández Ruiz: Conceptualization, Formal analysis, Writing – review & editing, Supervision, Project administration, Funding acquisition. Aurelio Muttoni: Conceptualization, Writing – review & editing, Supervision, Project administration, Funding acquisition.

# **Declaration of Competing Interest**

The authors declare that they have no known competing financial interests or personal relationships that could have appeared to influence the work reported in this paper.

# Acknowledgements

The authors would like to sincerely acknowledge the support given by the association of the Swiss cement producers (cemsuisse, research grant nr. 201801) for the financial support and technical discussions. The authors also thank the material supply by Lafarge-Holcim

Switzerland (mortar) and S&P (carbon textiles).

#### Annex A: Derivation of the safety format proposals for TRC structures

In this annex, the methodology used for the safety format calibration of TRC structures is presented. The annex is based on the semi-probabilistic reliability verification approach of the Eurocodes [9]. To that aim, the target reliability index  $\beta_{tgt}$  provided in EN1990:2002 [9] for structures with medium consequence class and a reference period of 50 years at the ultimate limit state is used ( $\beta_{tgt} = 3.8$ ).

The partial factors used in the semi-probabilistic reliability verification approach of the Eurocodes [9] are calibrated based on the First Order Reliability Method (FORM) [20,45]. Based on the FORM, to achieve the target reliability level, the partial factor for each basic random variable can be defined with the aid of the FORM sensitivity factors, which are the directional cosines of the vector between the mean value point and the FORM design point in standardised normal space.

In principle, independently of the type of safety format selected, the required partial factors to achieve the exact target reliability level are different for each individual case due to the difference in the shape of the limit state function. The shape of the limit state function depends on the mechanical model of the corresponding limit state as well as the probabilistic modelling of the basic uncertainties involved in the limit states. However, to simplify the design procedure, in the semi-probabilistic approach, the values of the partial factors are fixed and selected with the criterion that the achieved reliability level for representative design cases are as close as possible to the target value. Another important simplification in the safety format calibration in Eurocodes is to adopt standardised FORM sensitivity factors for the resistance variable and the action effect variable. The FORM sensitivity factor for the resistance  $\alpha_R$  is assumed to take the value of 0.8 and that for the action effect  $\alpha_E$  is assumed to take the value of -0.7 provided that the ratio between the standard deviation of the action effect variable and the resistance variable is within the range of 0.16 to 7.6 [9]. Using these standardised values makes it possible to separate the task of calibrating the partial safety factors on the resistance side and on the action effect side, which largely simplified the safety format calibration procedure. On the basis of such simplification, the target for the calibration of the partial factors for the resistance of TRC structures becomes:

$$Prob(R - R_d < 0) = \Phi(-\alpha_R \beta_{tot}) \tag{A.1}$$

When using the FORM or other reliability methods to calibrate the partial factors, iterative procedures are usually needed. However, under some conditions, simple analytical solutions can be derived for the partial factors. This can be done by making reasonable assumptions about the form of the limit state function. The resulting partial factors can eventually then be verified with the FORM or full-probabilistic reliability methods for the representative design cases. This strategy will be followed in this work when calibrating the safety format for TRC structures.

Considering the basic random variables involved in the resistance of TRC structures, the general form of the resistance function can be assumed as:

$$R = \theta_{R,local}R(f_{tex}, f_c, d) \tag{A.2}$$

The specific form of the resistance function depends on mechanical model of the resistance and also the values of the basic variables.

For calculation of the bending resistance of TRC structures, the methodology presented in Section 3 is considered, based on the Bernoulli-Navier assumption. The resistance of a cross section can be controlled either by the tensile strength of the textile reinforcement or by the compressive strength of concrete (but not by the two material strengths at the same time). The cases where the resistance is controlled by concrete strengths are not within the scope of this paper, as they are similar to conventional over-reinforced concrete structures, and the safety elements for this type of cases are actually applied through the partial factor on concrete compressive strength. For the cases where the resistance is controlled by the textile reinforcement, Eq. (A.2) can be further simplified to the following form:

$$R = \theta_{R,local}R(f_{lex}, d) \tag{A.3}$$

It is then reasonable to make an additional assumption considering that the resistance can be approximated by a multiplicative form of the basic random variables:

$$R = \theta_{R,local} R(f_{tex}, d) \approx A_R \theta_{R,local} f_{tex} d$$
(A.4)

Where  $A_R$  represents a coefficient that depends on the other deterministic parameters related to the resistance. Based on the assumption in Eq. (A.4), the CoV of the resistance  $V_R$  can be calculated approximately as:

$$V_R \approx \sqrt{V_{\theta_R}^2 + V_{f_{\text{ex}}}^2 + V_d^2} \tag{A.5}$$

It should be noted that Eq. (A.5) would be a close approximation if all the basic variables follow lognormal distributions, but in this case the flexural depth d is modelled as a normally distributed variable. In any case, Eq. (A.5) can still be a reasonable approximation for the purpose of estimating the partial factors. The validity of the above assumptions will eventually be verified by reliability analysis of representative cases with the selected partial factors.

With respect to the value of  $V_d$ , it depends on the nominal flexural depth, and this results in different values of  $V_R$  for cases with different flexural depths. For instance, for the range of  $d_{nom} = 15$ –60 mm, the approximated value of  $V_R$  is plotted in Fig. A.1a.

Following the same strategy, the FORM sensitivity factors for the basic variables can also be estimated as follows:

$$lpha_{flex} pprox \sqrt{rac{V_{f_{lex}}^2}{V_{ heta_R}^2 + V_{f_{lex}}^2 + V_d^2}}$$
 (A.6)

$$lpha_{ heta_R} pprox \sqrt{rac{V_{f_{ heta_R}}^2}{V_{ heta_R}^2 + V_{f_{c...}}^2 + V_{d}^2}}$$
 (A.7)

$$\alpha_d \approx \sqrt{\frac{V_{f_d}^2}{V_o^2 + V_c^2 + V_d^2}} \tag{A.8}$$

The change of the FORM sensitivity factors with the flexural depth is plotted Fig. A.1b. It should be stressed that the above analysis is based on two approximations: the assumption that the resistance can be approximated as a multiplicative form of the basic variables and the assumption that the resistance can be approximated by a lognormal distribution. From this analysis, it can be observed that the FORM sensitivity factor for the flexural

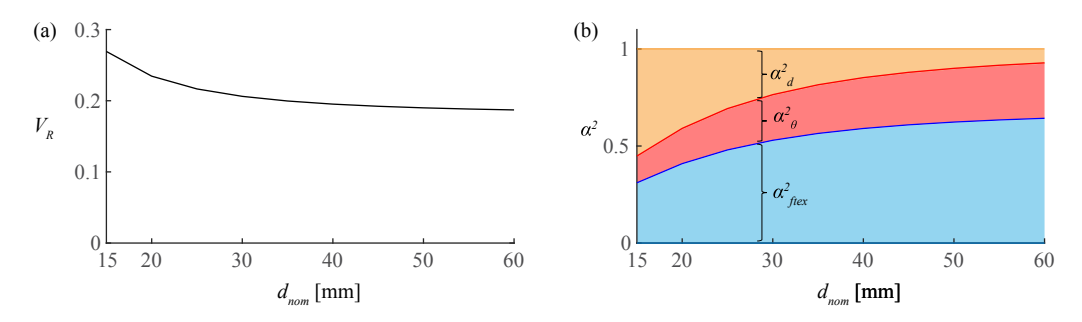


Fig. A1. Analysis of the influence of  $d_{nom}$ : (a)  $V_R$ ; and (b) FORM senstivity factors.

depth decreases with increasing depth. It can further be observed that for the cases where the mean value of the flexural depth is relatively small, its uncertainty becomes dominant. Since the flexural depth follows a normal distribution (see Table 8), in the cases when the uncertainty of the flexural depth is dominating, the assumption that the resistance follows lognormal can be not valid anymore. This means the estimated FORM sensitivity factors of the range where the flexural depth is small can deviate from the actual value. Nevertheless, the estimated values can still provide important information for the safety format calibration problem and can be used as a useful reference. The estimated values of the CoV of the resistance variable and the FORM sensitivity factors of basic variables are used in the safety format calibration in Section 7 and their effectiveness is eventually verified by reliability analysis of representative cases.

# Annex B: Analysis of an assembled cross-beam system

The aim of this annex is to provide a detailed example of the assembled cross-beam system, following the procedure explained in Section 5. The assembled cross-beam composed of beam TB1 and TB8 is used for this purpose. For beam TB1 (refer to Section 3 for the values of the parameters of beam TB1), the uncracked cross-sectional flexural stiffness  $EI_{UC}$  is:

$$EI_{UC} = E_{cm} \frac{bh^3}{12} = 1.40 \cdot 10^8 [\text{kN} \cdot \text{mm}^2]$$
 (23)

Thus, the uncracked stiffness of the beam TB1 results:

$$\left(\frac{dQ}{d\delta}\right)_{LAUC} = \frac{48EI_{UC}}{L^3} = 3.88[kN/mm] \tag{24}$$

And the cracked cross-sectional flexural stiffness  $EI_{FC}$  of beam TB1 is:

$$EI_{FC} = \frac{bx_N^3}{3}E_{cm} + \sum_{i=1}^{n_r} (d_i - x_N)^2 a_{tex}E_{tex,m} = 1.13 \cdot 10^7 [\text{kN} \cdot \text{mm}^2]$$
(26)

Where  $x_N$  refers to the position of the neutral axis (see Fig. 5) and the fully-cracked stiffness of beam TB1 is:

$$\left(\frac{dQ}{d\delta}\right)_{LAFC} = \frac{48EI_{FC}}{L^3} = 0.31[\text{kN/mm}] \tag{27}$$

The uncracked and fully-cracked stiffness of beam TB8 can be calculated with the same method. Based on this information, the load-deflection curves of the assembled system using LAUC and LAFC methods are calculated and plotted in Fig. B.1. For the NLA, a trilinear moment-curvature relationship is assumed for each beam and the actual extent of cracked and uncracked regions are accounted for. The resultant response of the assembled system using NLA method and the assembled experimental response are plotted in Fig. B1. for the selected case.

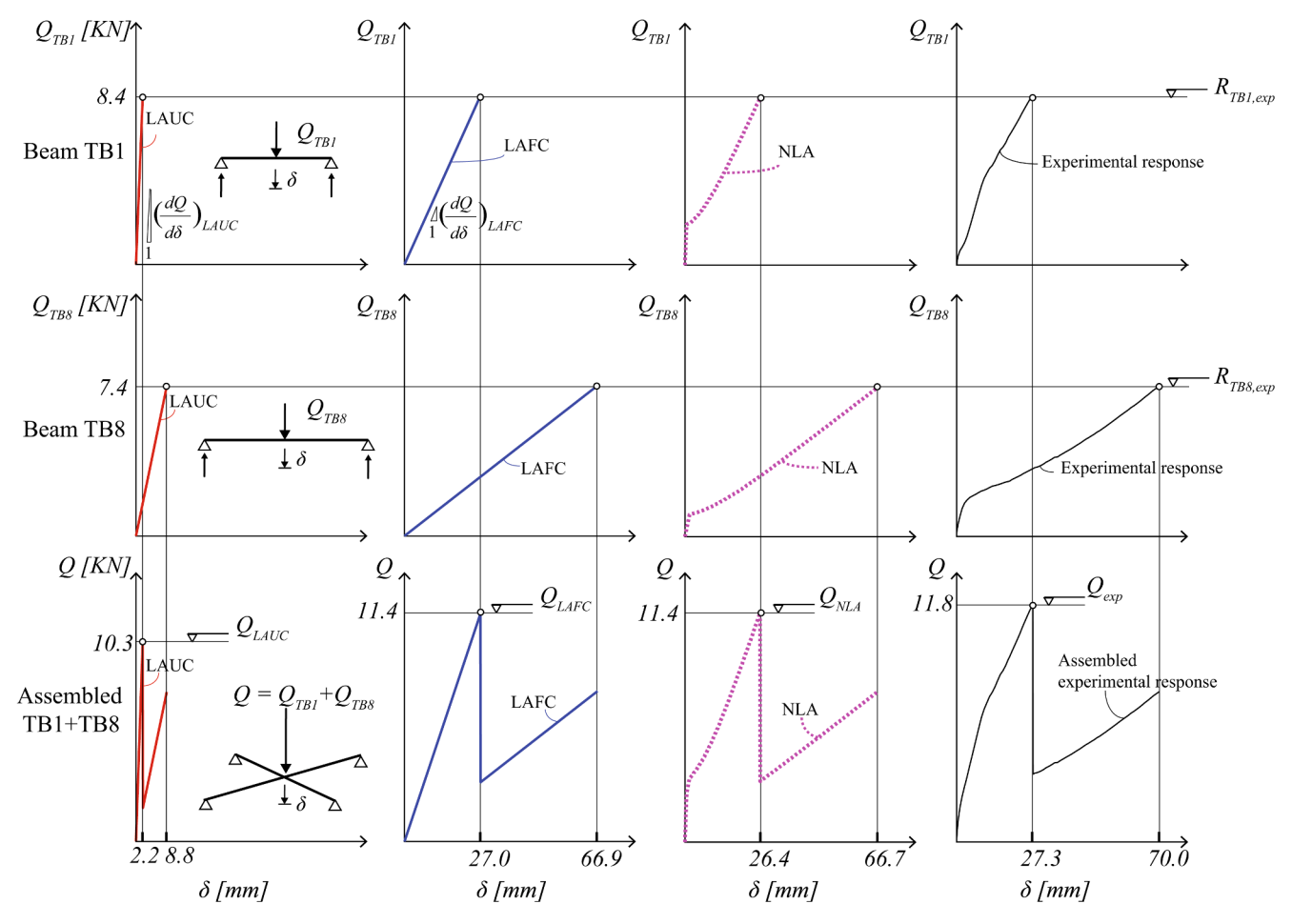


Fig. B1. Response of the assemble cross-beam system composed of beam TB1 and TB8.

### References

- [1] Zhen He, Wen-quan L, Bei-xing Li, Xiang-guo Li. Preparation of super composite cement with a lower clinker content and a larger amount of industrial wastes. J Wuhan Univ Technol Mater Sci Ed 2002;17(4):78–81. https://doi.org/10.1007/ BF02838424.
- [2] Garcia-Lodeiro I, Fernández-Jimenez A, Palomo A. Cements with a low clinker content: versatile use of raw materials. J Sustain Cem Mater 2015;4(2):140–51. https://doi.org/10.1080/21650373.2015.1040865.
- [3] Valeri P, Guaita P, Baur R, Fernández Ruiz M, Fernández-Ordóñez D, Muttoni A. Textile reinforced concrete for sustainable structures: Future perspectives and application to a prototype pavilion. Struct Concr J FIB 2020;21(6):2251–67.
- [4] Reinhardt, H-W, Raupach, M, Orlowsky, J. MK. Behavior of Textile-Reinforced Concrete in Fire. ACI Symp Publ n.d.;250. DOI: 10.14359/20143.
- [5] Colombo I, Colombo M, Magri A, Zani G, di Prisco M. Textile Reinforced Mortar at High Temperatures. Appl Mech Mater 2011;82:202–7. https://doi.org/10.4028/ www.scientific.net/AMM.82.202.
- [6] Ehlig D, Jesse F, Curbach M. High temperature tests on textile reinforced concrete (TRC) strain specimens. In: 2nd ICTRC Text Reinf Concr Proc Int RILEM Conf Mater Sci 2010;1:141–51.
- [7] Brameshuber W. Textile reinforced concrete-state-of-the-art report of RILEM TC 201-TRC. 2006.
- [8] Peled A. Textile reinforced concrete . Boca Raton, Florida ; CRC Press; 2017.
- [9] CEN. EN 1990:2002: Eurocode: Basis of Structural Design. Brussels: 2002.
- [10] CEN. EN 1992-1-1:2004: Eurocode 2: Design of concrete structures Part 1-1: General rules and rules for buildingsle. Brussels: 2004.
- [11] Fédération Internationale du Béton. fib Model Code for Concrete Structures 2010. Berlin, Germany, 434 P.: Ernst & Sohn; 2013.
- [12] Rempel S. Zur Zuverlässigkeit der Bemessung von biegebeanspruchten Betonbauteilen mit textiler Bewehrung. Aachen, Germany: Aachen University; 2019.
- [13] Rempel S, Ricker M, Hegger J. Safety Concept for Textile-Reinforced Concrete Structures with Bending Load. Appl Sci 2020;10(20):7328. https://doi.org/ 10.3390/app10207328.
- [14] Just M. Sicherheitskonzept für Textilbeton. Beton- Und Stahlbetonbau 2015;110 (S1):42–6. https://doi.org/10.1002/best.201400109.
- [15] Weselek J, Häußler-Combe U. Calibrating safety factors for Carbon Concrete. Beton- Stahlbetonbau 2018;113:14–21. https://doi.org/10.1002/best.201800056.

- [16] Häußler-Combe U, Weselek J, Jesse F. A Safety Concept for Non-Metallic Reinforcement for Concrete under Bending. ACI Struct J 2019;116. https://doi. org/10.14359/51710873.
- [17] Kromoser B, Preinstorfer P, Kollegger J. Building lightweight structures with carbon-fiber-reinforced polymer-reinforced ultra-high-performance concrete: Research approach, construction materials, and conceptual design of three building components. Struct Concr J FIB 2019;20(2):730–44. https://doi.org/10.1002/ suco.201700225.
- [18] CEN. prEN 1990:2020: Eurocode: Basis of structural and geotechnical design 2020.
- [19] Engen M, Hendriks MAN, Köhler J, Øverli JA, Åldstedt E. A quantification of the modelling uncertainty of non-linear finite element analyses of large concrete structures. Struct Saf 2017;64:1–8. https://doi.org/10.1016/j. strusafe 2016 08 003
- [20] Hasofer AM, Lind NC. Exact and invariant second-moment code format. J Eng Mech Div 1974;100(1):111–21.
- [21] König G, Hosser D. The simplified level II method and its application on the derivation of safety elements for level I. CEB Bull 1982.
- [22] Nielsen MP, Hoang LC. Limit analysis and concrete plasticity. third edition; 2016.
- [23] Muttoni A. Die Anwendbarkeit der Plastizitätstheorie in der Bemessung von Stahlbeton, vol. 176. Basel: Birkhäuser Basel; 1990.
- [24] CEB. Practical unified recommendations for the design and execution of structures in reinforced concrete (in French: Recommendations pratiques unifiées pour le calcul et l'éxécution des ouvrages en béton armé). Paris: CEB; 1964.
- [25] CEB. Bulletin CEB 19: Technical conclusions of the 5th CEB meeting in Vienna Bulletin: Section on Structural Safety. CEB; 1959.
- [26] Manuel CEB. "sécurite des structures": concepts généraux, charges et actions. Paris: CEB; 1974.
- [27] Manuel CEB. de calcul "flambement instabilité". Paris: CEB; 1974.
- [28] Manuel CEB. "sécurité des structures": concepts généraux, actions, combinaisons et sollicitations agissantes résistances et sollicitations résistantes, états-limites divers et situations diverses, règles générales d'application. 2 ème éd. Paris: CEB; 1980.
- [29] Valeri P, Fernàndez Ruiz M, Muttoni A. Tensile response of textile reinforced concrete. Constr Build Mater 2020;258:119517. https://doi.org/10.1016/j. conbuildmat.2020.119517.
- [30] Fédération Internationale du Béton (fib). FRP reinforcement in RC structures. Lausanne: Fédération Internationale du Béton fib; 2007. DOI: DOI: doi.org/10.35789/fib.BULL.0040.

- [31] Hawkins W, Orr J, Ibell T, Shepherd P. An Analytical Failure Envelope for the Design of Textile Reinforced Concrete Shells. Structures 2018;15:56–65. https:// doi.org/10.1016/j.istruc.2018.06.001.
- [32] Preinstorfer P, Kromoser B, Kollegger J. Flexural behaviour of filigree slab elements made of carbon reinforced UHPC. Constr Build Mater 2019;199:416–23. https://doi.org/10.1016/j.conbuildmat.2018.12.027.
- [33] Williams Portal N, Nyholm Thrane L, Lundgren K. Flexural behaviour of textile reinforced concrete composites: experimental and numerical evaluation. Mater Struct 2016;50:4. https://doi.org/10.1617/s11527-016-0882-9.
- [34] Hegger J, Will N. 8 Textile-reinforced concrete: Design models. In: Triantafillou TBT-TFC in CE, editor., Woodhead Publishing; 2016, p. 189–207. DOI: https://doi. org/10.1016/B978-1-78242-446-8.0009-4.
- [35] Tysmans T, Adriaenssens S, Cuypers H, Wastiels J. Structural analysis of small span textile reinforced concrete shells with double curvature. Compos Sci Technol 2009; 69(11-12):1790–6. https://doi.org/10.1016/j.compscitech.2008.09.021.
- [36] Schladitz F, Frenzel M, Ehlig D, Curbach M. Bending load capacity of reinforced concrete slabs strengthened with textile reinforced concrete. Eng Struct 2012;40: 317–26. https://doi.org/10.1016/j.engstruct.2012.02.029.
- [37] Phoenix S., Taylor HM. The asymptotic strength distribution of a general fiber bundle. Adv Appl Probab 1973;5(2):200–16.

- [38] Chudoba R, Vořechovský M, Konrad M. Stochastic modeling of multi-filament yarns. I. Random properties within the cross-section and size effect. Int J Solids Struct 2006;43(3-4):413–34.
- [39] Vořechovský M, Chudoba R. Stochastic modeling of multi-filament yarns: II. Random properties over the length and size effect. Int J Solids Struct 2006;43(3-4): 435–58.
- [40] Valeri P, Ruiz MF, Muttoni A. cemsuisse report 201407: Building in a lighter and more sustainable manner: textile reinforced concrete for thin structural elements. Lausanne 2017.
- [41] Valeri Patrick, Ruiz Miguel Fernández, Muttoni Aurelio. Modelling of Textile Reinforced Concrete in bending and shear with Elastic-Cracked Stress Fields. Eng Struct 2020;215:110664. https://doi.org/10.1016/j.engstruct.2020.110664.
- [42] Schneider J. Introduction to safety and reliability of structures. vol. 5. 3rd review. Zürich: International Association for Bridge and Structural Engineering IABSE; 2017
- [43] JCSS. Probabilistic Model Code. 2001.
- [44] CEN. prEN 1992-1-1: 2020: Eurocode 2: Design of concrete structures Part 1-1: General rules - Rules for buildings, bridges and civil engineering structures 2020: 463.
- [45] Madsen HO, Krenk S, Lind NC. Methods of structural safety. Englewood Cliffs, N. J. Prentice-Hall; 1986.